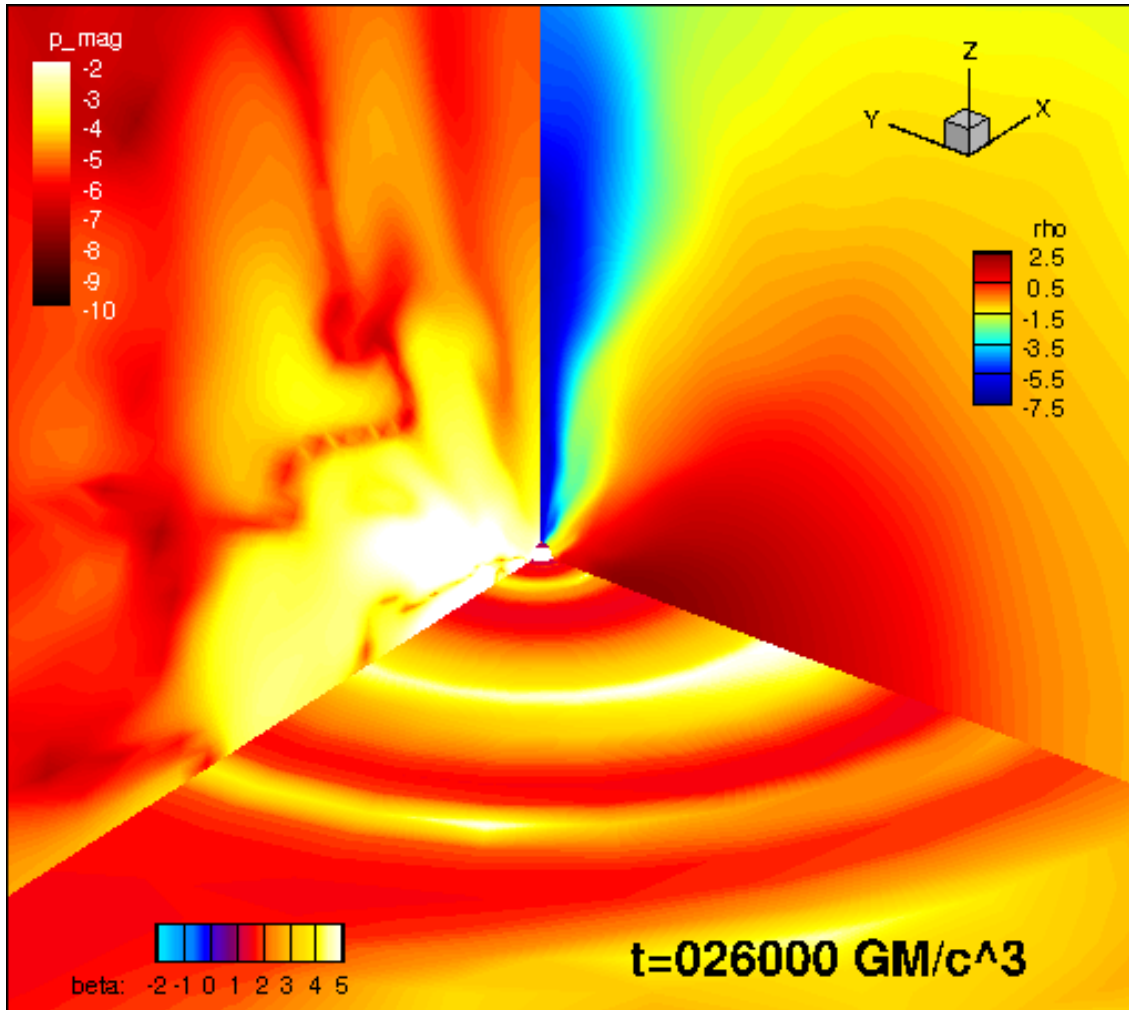


3D-GRMHD simulation of black hole and accretion disk



Akira MIZUTA(RIKEN)

Toshikazu Ebisuzaki (RIKEN)

Toshiki Tajima (UCI)

Shigehiro Nagataki (RIKEN)

第9回『ブラックホール磁気圏
勉強会』研究会

2016.03.25@

マウントレースイホテル

OUTLINE

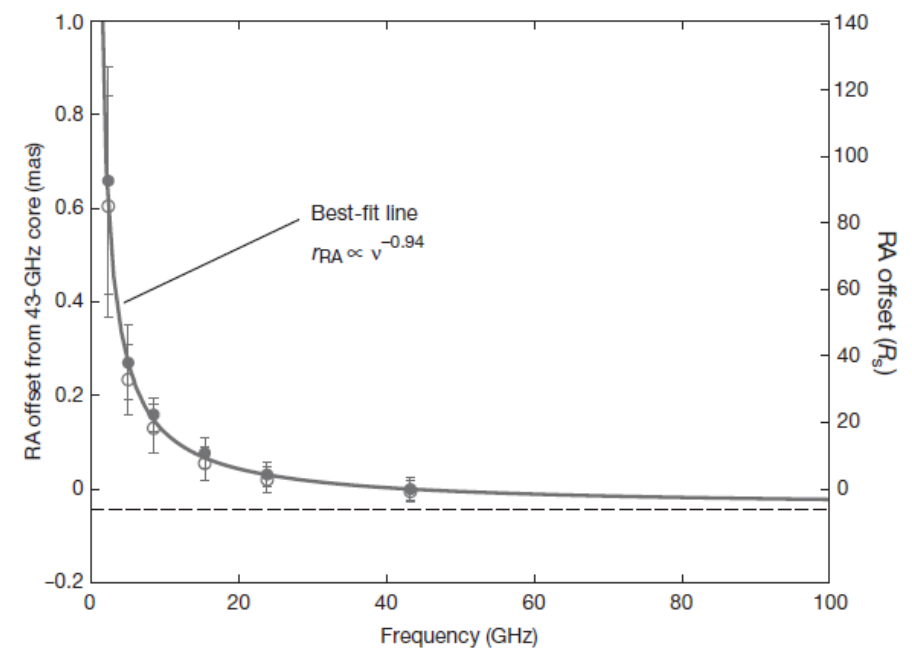
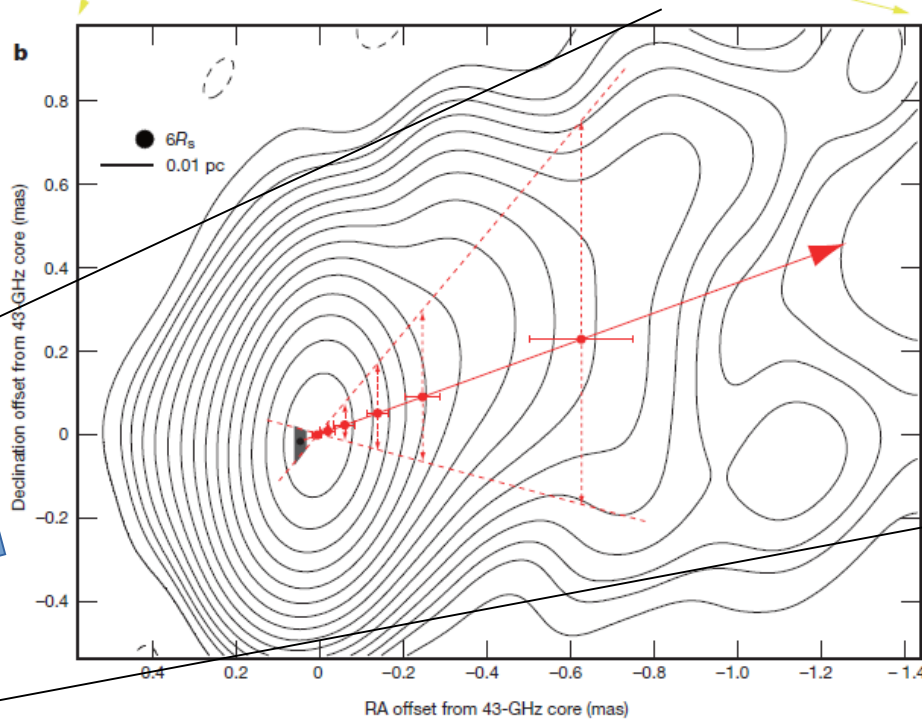
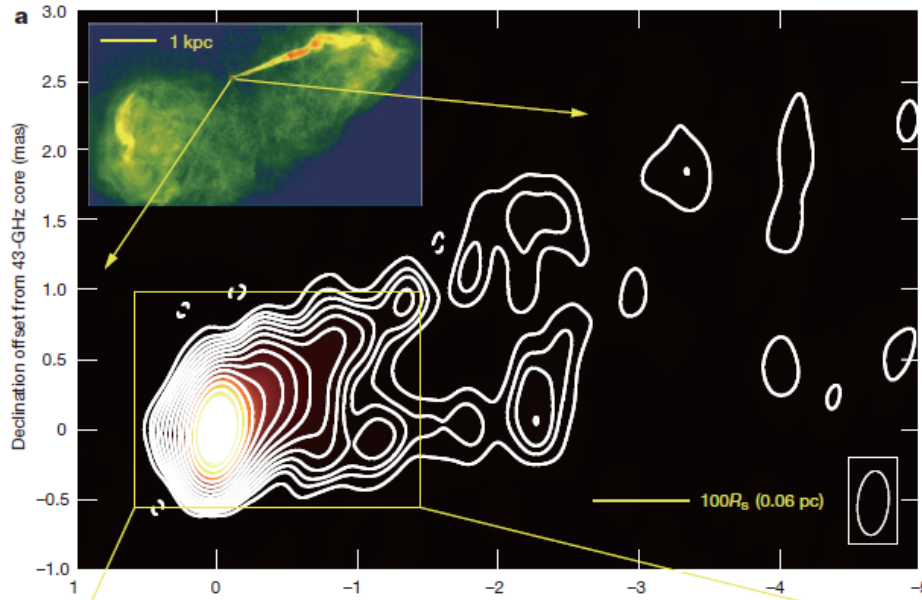
- Introduction: observations of AGN jets
- GRMHD simulations of black hole and accretion disks
 - Blandford-Znajek process
 - bulk acceleration outflows
- Initial condition
- Particle acceleration by wakefield acceleration
- Summary

Introduction

observations of AGN jets

M87 radio observations

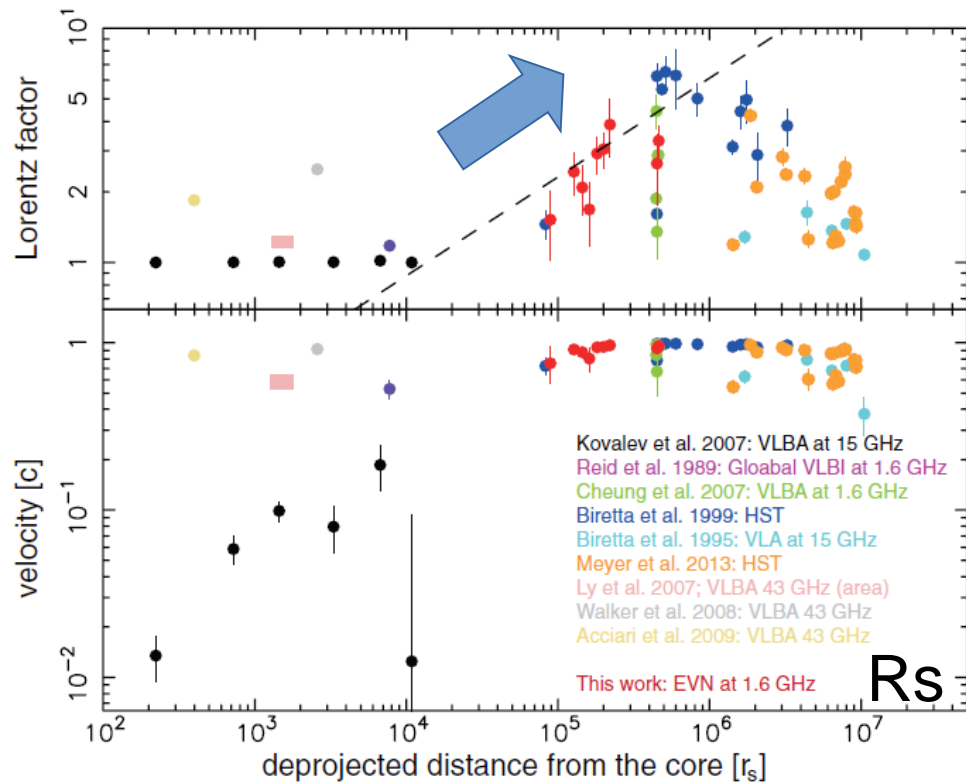
- M87 $D=16.7\text{Mpc}$
- $M_{\text{BH}} \sim 3.2\text{-}6.6 \times 10^9 M_{\text{sun}}$
- Location of the central BH is near the radio core by analysis of several bands of radio observations.
- It is consistent that the shape of the jet near the core is not conical but parabolic.
- Rim brightening @ $100R_s$



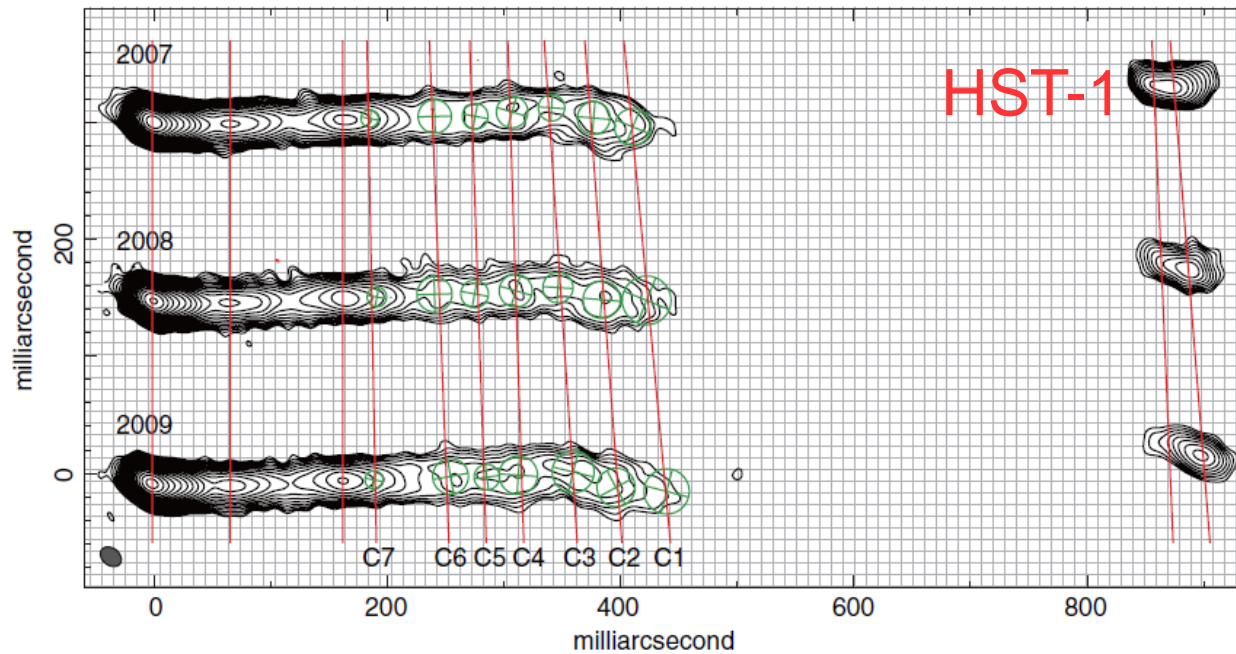
M87 radio observation Hada +(2011)

BH?
No!

Where is acceleration site ?

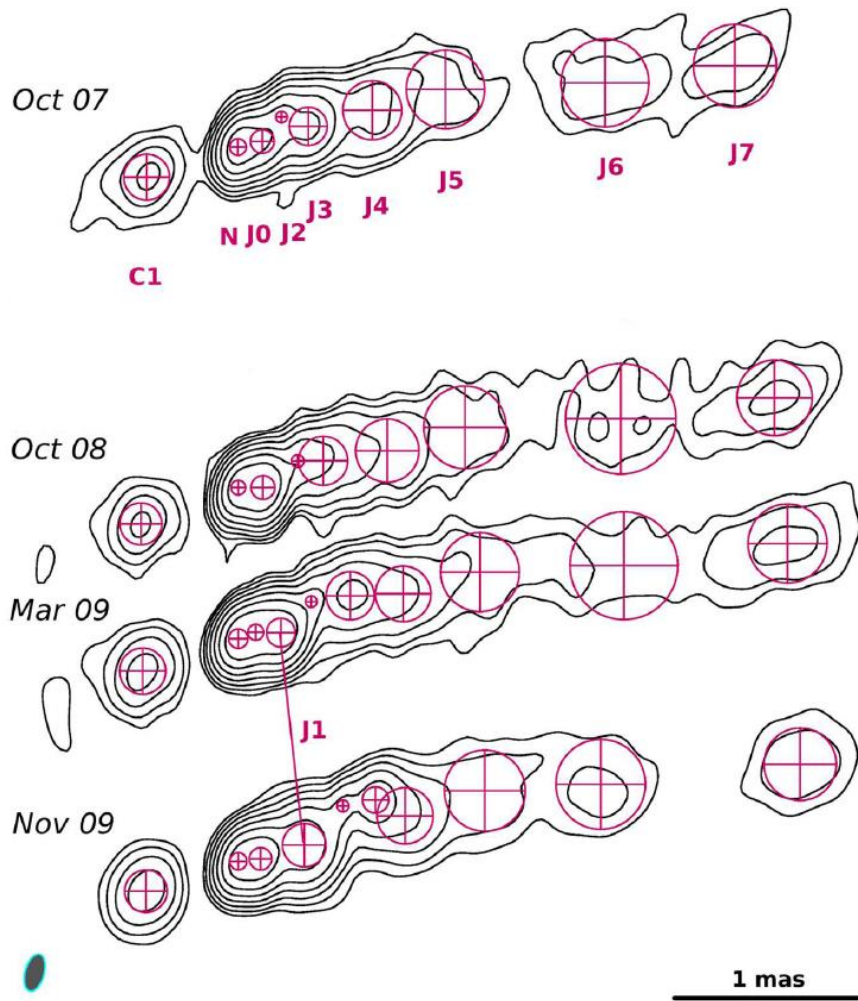


- Bulk velocities are measured by using a series of radio observations of M87 up to $10^{5-6} R_s$.
- Acceleration to relativistic velocities occurs at $\sim 10^4 R_s$.
- Similar results for Cygnus A jets. (Boccardi + A&A (2016))

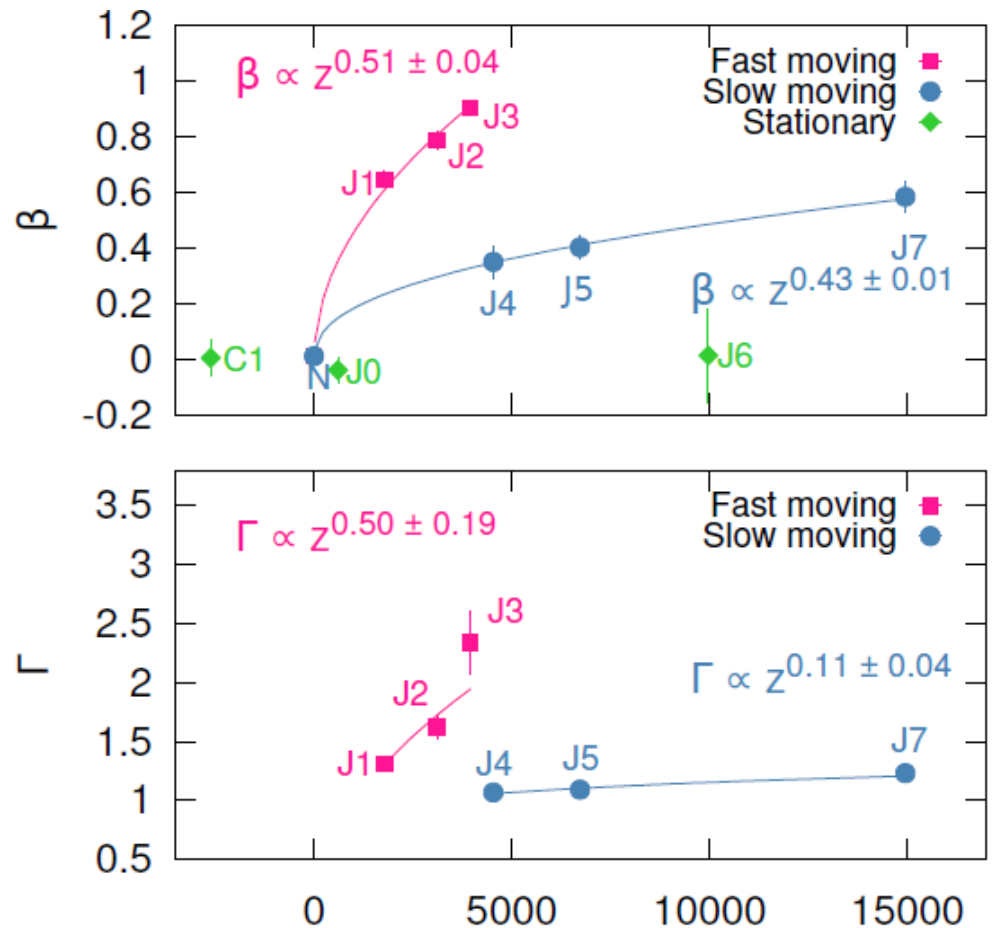


Asada +2014

High resolution radio observation resolves structured of the jet near the core (Cygnus A)



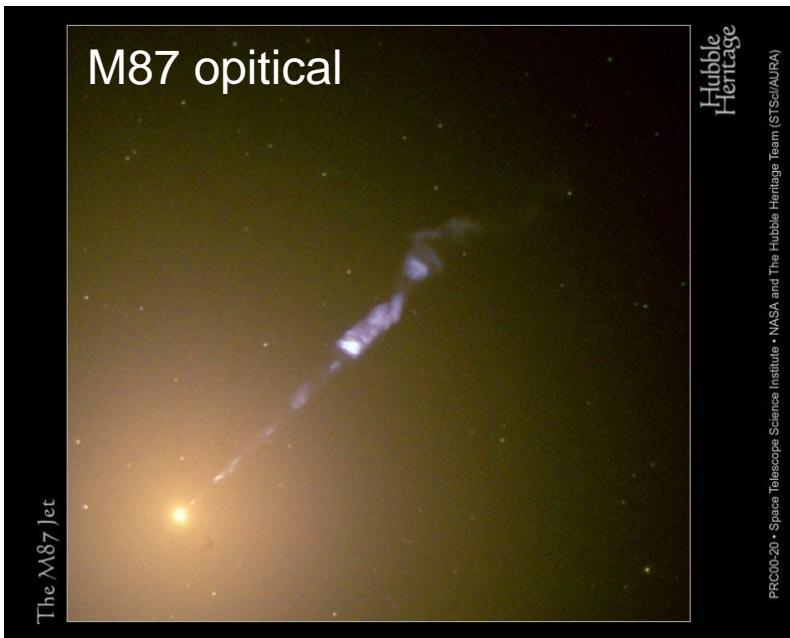
Boccardi + A&A (2016)



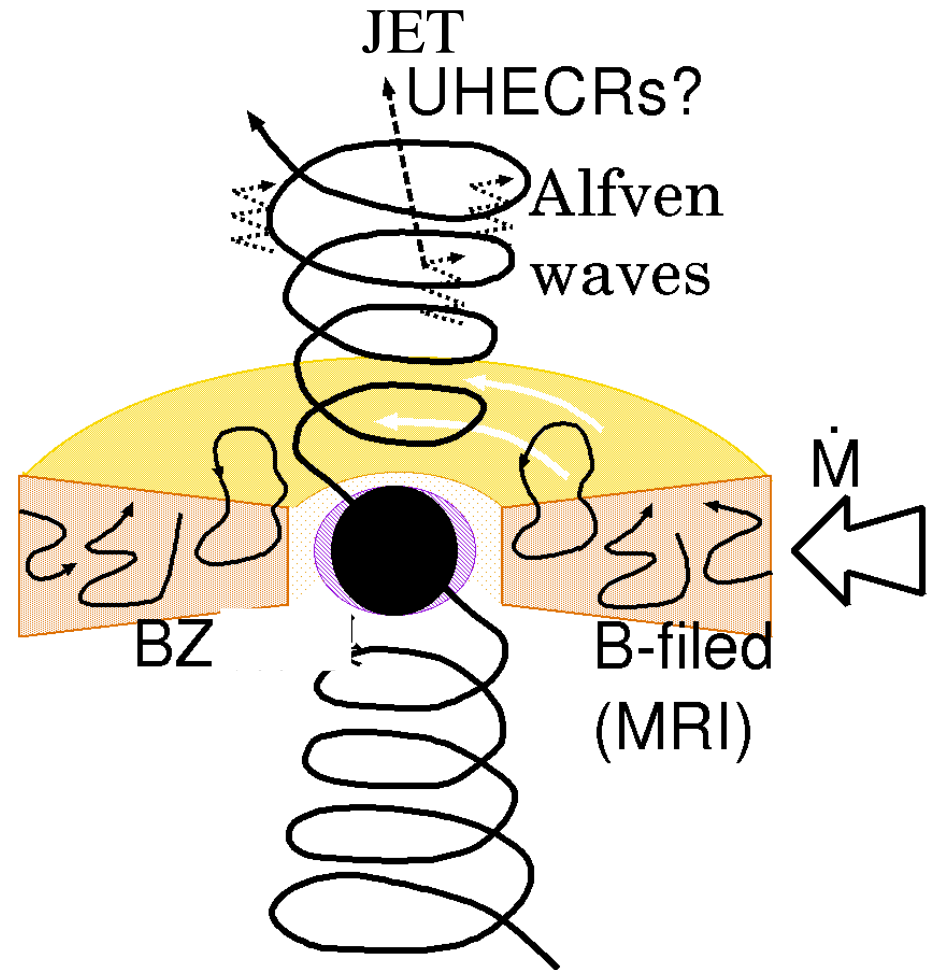
De-projected z [r_s]
 Cygnus A jet (FR II)
 $z=0.056$, $1 \text{ mas} = 1.084 \text{ pc}$
 $M_{\text{BH}} = 2.5 \times 10^9 M_{\text{sun}}$

Blazar observations (3C279, etc) show minute scale time variability in sub TeV γ rays $\Rightarrow \Gamma \sim 50$ @ 100rg (Hayashida+2016)

Relativistic jet launched from BH+accretion disk



- Central Engine
 - Black Hole(BH) + accretion disk
 - B filed amplification
- relativistic jet ($\Gamma \sim 10$ for AGN jet)
 - How to launch the jet is also a big problem for astrophysics.
 - Blandford-Payne (magnetic centrifugal force)
 - Blandford-Znajek (general relativistic + B filed effect)
 - or others ?



B filed plays an important role !

GRMHD simulations of Black hole and accretion disks

Basic Equations : GRMHD Eqs.

$GM=c=1$, a : dimensionless Kerr spin parameter

$$\frac{1}{\sqrt{-g}} \partial_\mu (\sqrt{-g} \rho u^\mu) = 0 \quad \text{Mass conservation Eq.}$$

$$\partial_\mu (\sqrt{-g} T_\nu^\mu) = \sqrt{-g} T_\lambda^\kappa \Gamma^\lambda_{\nu\kappa} \quad \text{Energy-momentum conservation Eq.}$$

$$\partial_t (\sqrt{-g} B^i) + \partial_j (\sqrt{-g} (b^i u^j - b^j u^i)) = 0 \quad \text{Induction Eq.}$$

$$p = (\gamma - 1) \rho \epsilon \quad \text{EOS } (\gamma=4/3)$$

Constraint equations.

$$\frac{1}{\sqrt{-g}} \partial_i (\sqrt{-g} B^i) = 0 \quad \text{No-monopoles constraint}$$

$$u_\mu b^\mu = 0 \quad \text{Ideal MHD condition}$$

$$u_\mu u^\mu = -1 \quad \text{Normalization of 4-velocity}$$

Energy-momentum tensor

$$T^{\mu\nu} = (\rho h + b^2) u^\mu u^\nu + (p_g + p_{\text{mag}}) g^{\mu\nu} - b^\mu b^\nu$$

$$p_{\text{mag}} = b^\mu b_\mu / 2 = b^2 / 2$$

$$b^\mu \equiv \epsilon^{\mu\nu\kappa\lambda} u_\nu F_{\lambda\kappa} / 2 \quad B^i = F^{*it}$$

GRMHD code (Nagataki 2009,2011)

Kerr-Schild metric (no singular at event horizon)

HLL flux, 2nd order in space (van Leer), 2nd or 3rd order in time

See also, Gammie +03, Noble + 2006

Flux-interpolated CT method for divergence free

Computational domain, grids

Spherical coordinate (r, θ, ϕ) $R[1.4:3e4]$ $\theta[0:\pi]$ $\phi[0:2\pi]$

$[Nr=124, N\theta=124, N\phi=28]$

$r=\exp(n_r)$, $d\theta\sim 1.5^\circ$, $d\phi\sim 13^\circ$: uniform

– not enough high resolution to resolve fastest MRI growth mode

Units $L : R_g=GM/c^2 (=R_s/2)$, $T : R_g/c=GM/c^3$, mass : scale free
 $\sim 1.5 \times 10^{13} \text{cm} (M_{\text{BH}}/10^8 M_{\text{sun}})$ $\sim 500 \text{s} (M_{\text{BH}}/10^8 M_{\text{sun}})$

Initial condition

Fisbone-Moncrief (1976) solution – hydrostatic solution of tori around rotating ($a=0.9$, $r_H\sim 1.44$), $l_* \equiv -u^t u_\phi = \text{const} = 4.45$, $r_{\text{in}}=6. > r_{\text{ISCO}}$

– equilibrium state : gravitational potential, pressure gradient, and centrifugal force, geometrical thick disk

– impose weak poloidal B-field (Minimum plasma beta = 100)

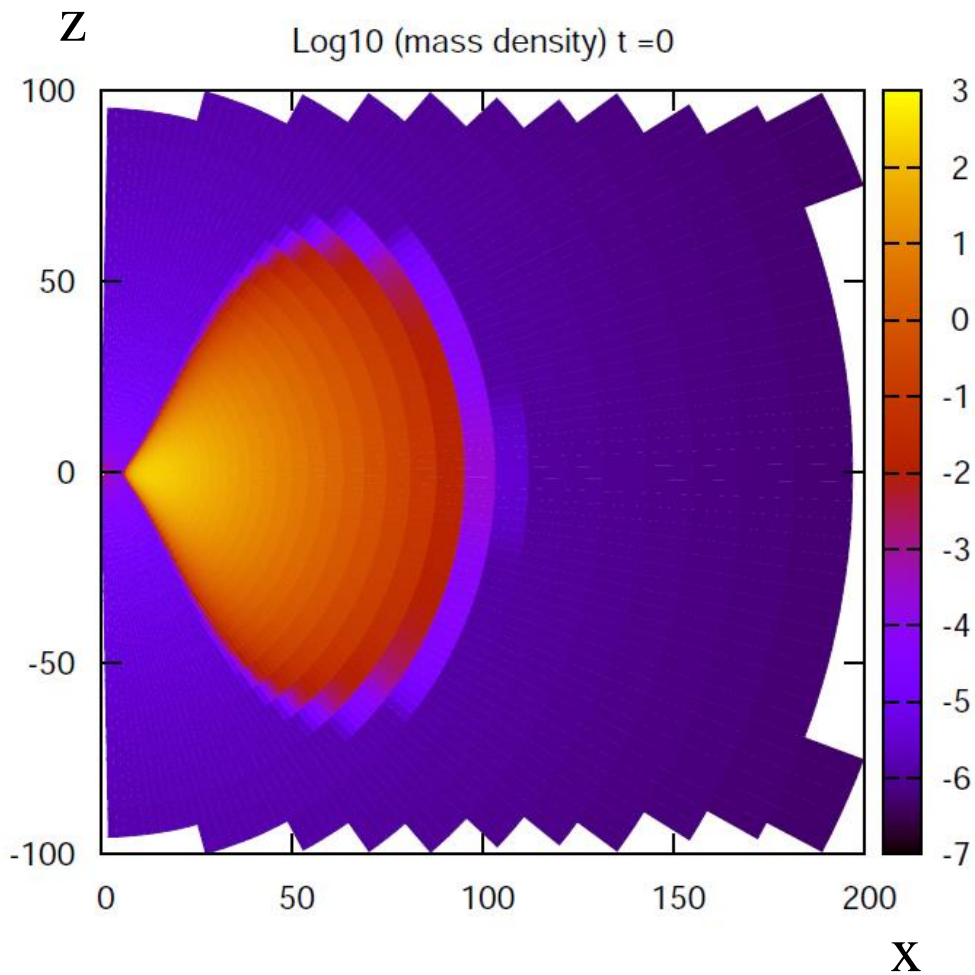
$$A_\phi \propto \max [\rho/\rho_{\text{max}} - 0.2, 0]$$

case1. maximum 5% random perturbation in thermal pressure (3D)

case2. w/o perturbation in thermal pressure (2D)

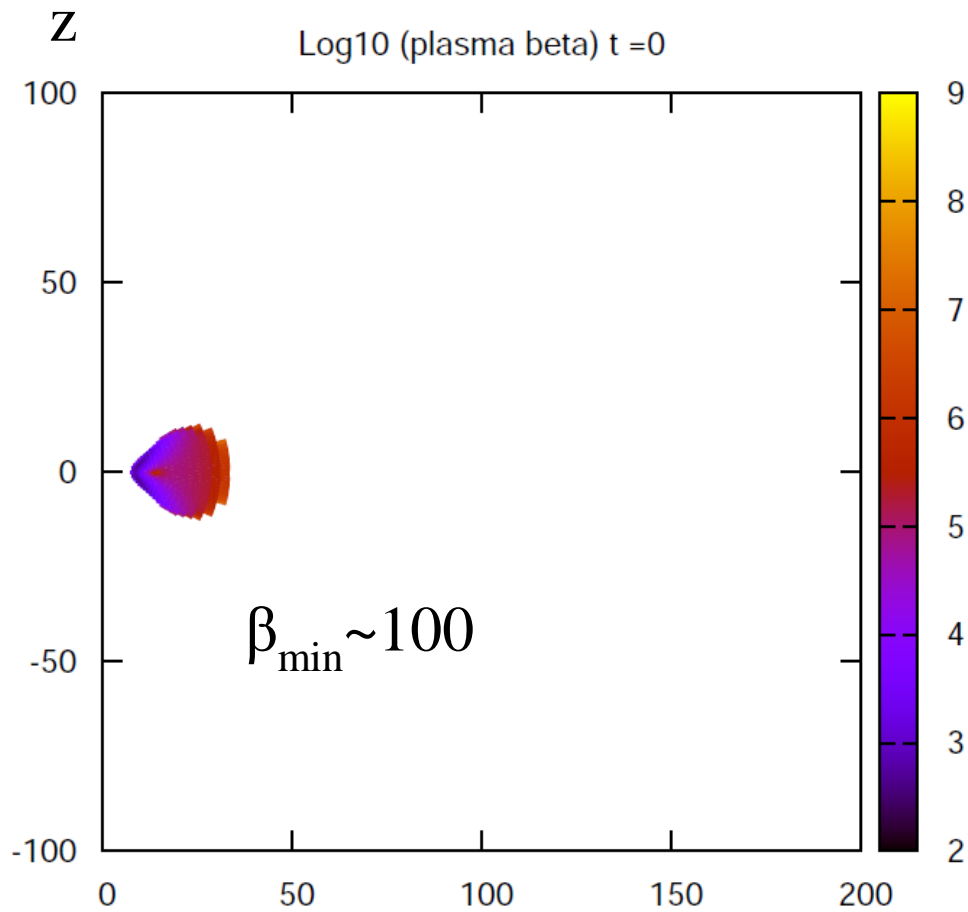
Initial Condition

Log10 (Mass density)



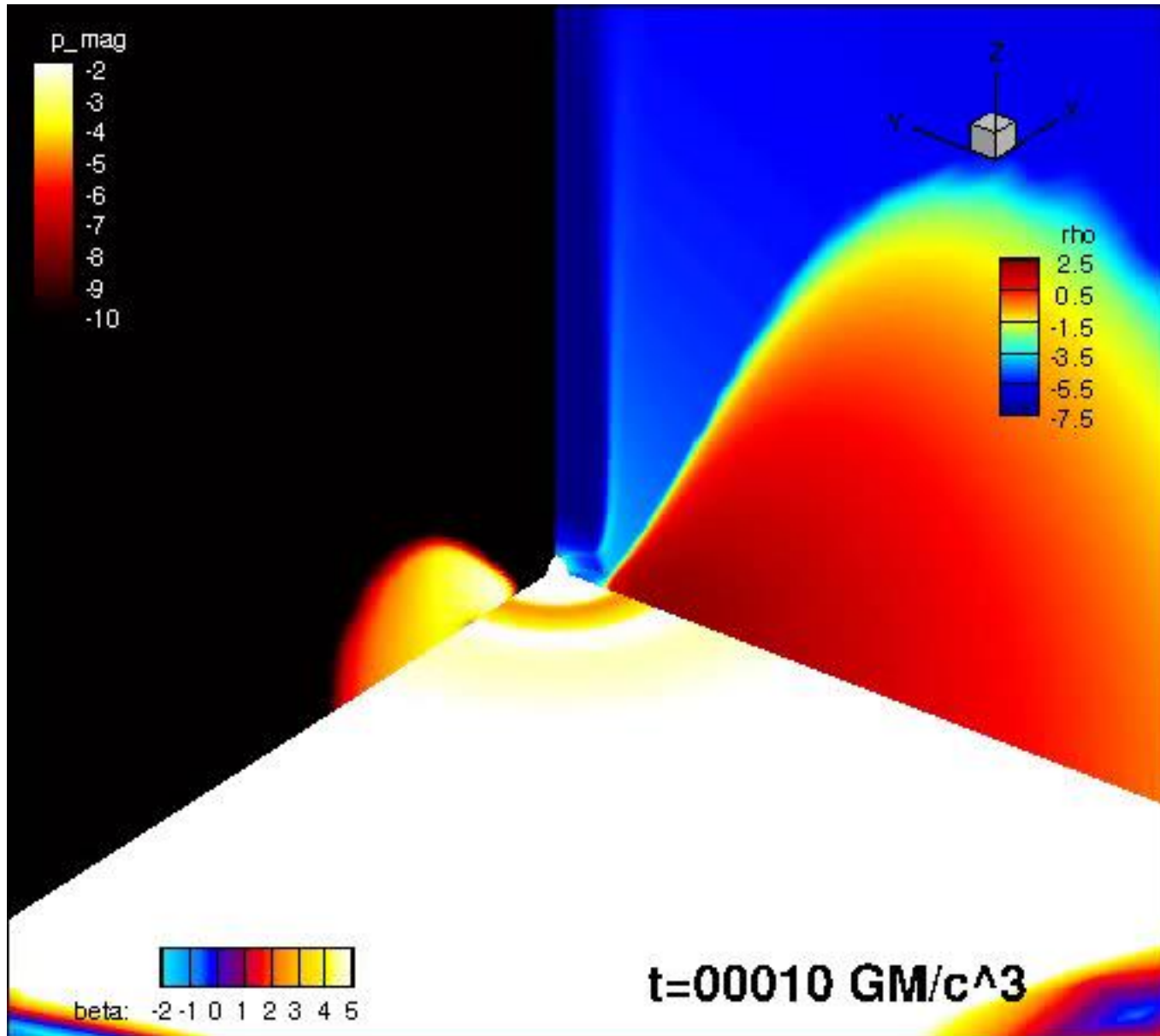
a=0.9,

Log10(Pgas/Pmag)



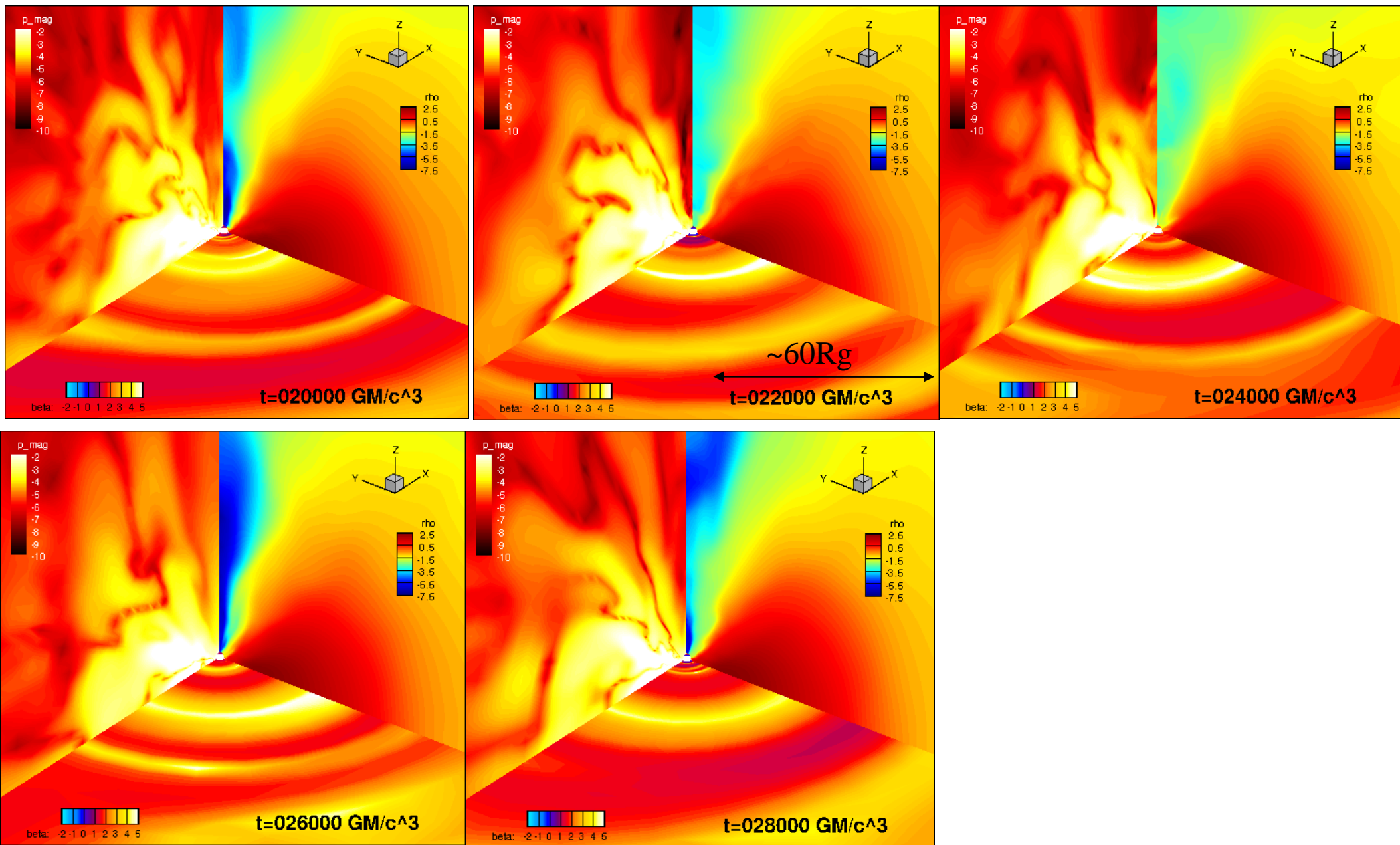
$$A_\phi \propto \max [\rho / \rho_{\max} - 0.2, 0]$$

Magnetized jet launch

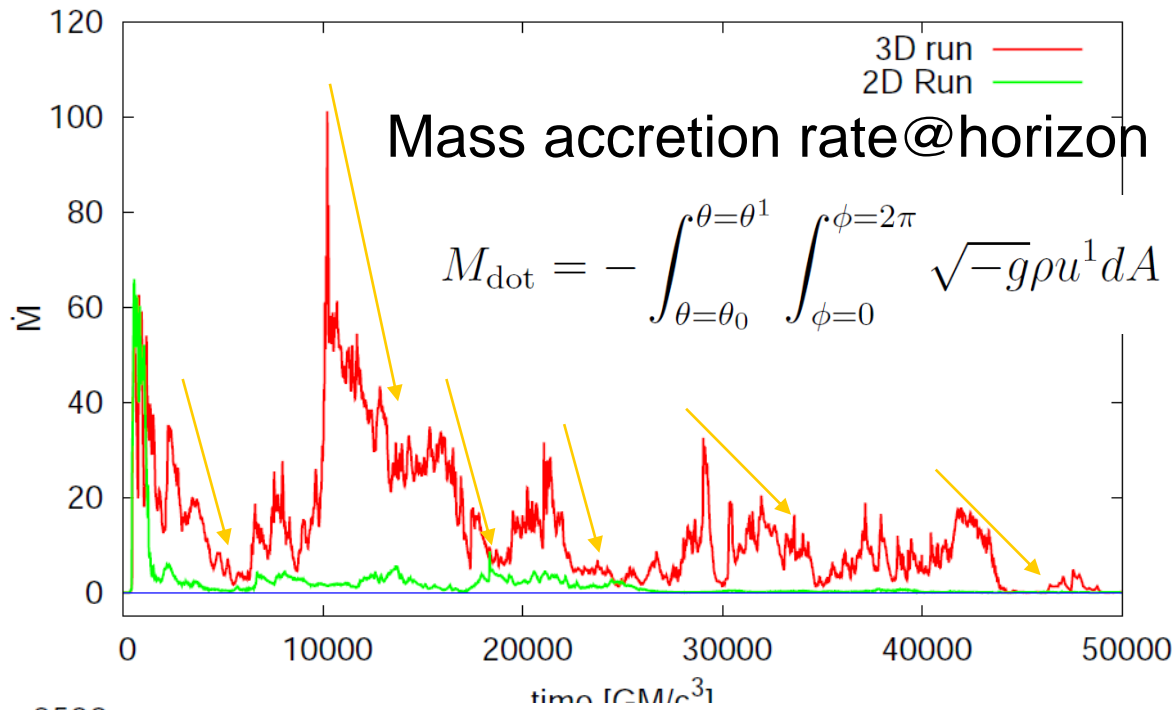


Low mass density and electromagnetic flux along the polar axis. Intermittent

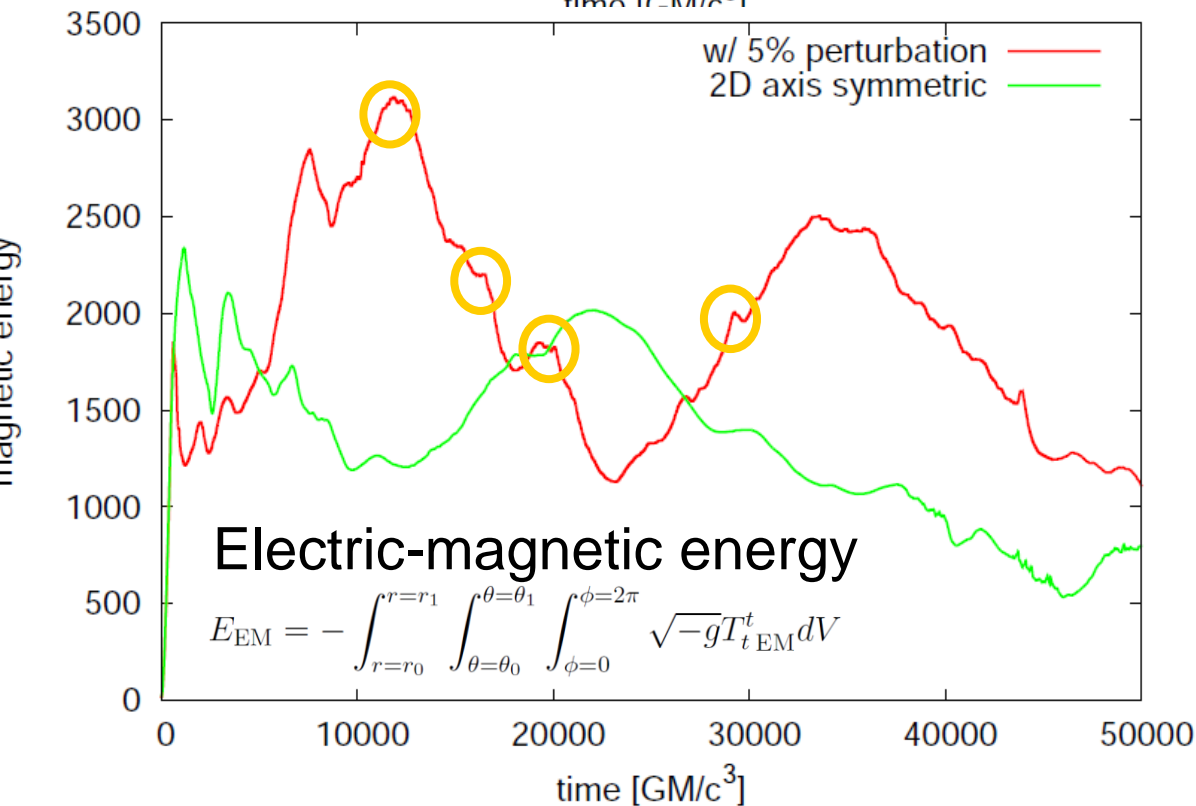
Magnetized jet launch



mass accretion rate $\dot{m}=1.4R_g$



- In transition phase (t < 18000 for 3D) accretion rate is relatively high.
- After that a new phase starts.
- Short time availability ($\Delta t \sim$ a few tens to a few hundreds.)
- Accretion rate for 2D is 1/10-1/100 lower than that of 3D.

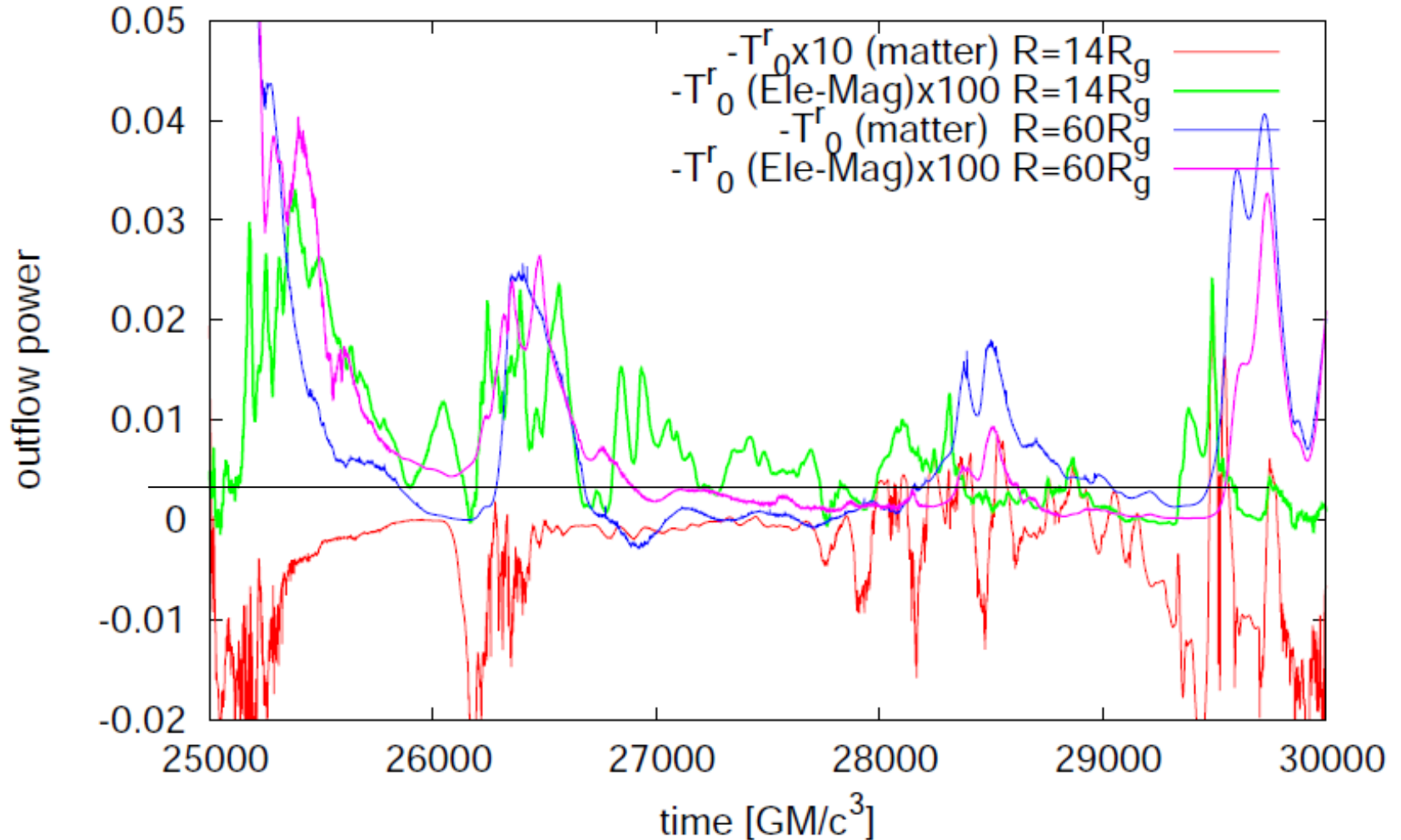


Outflow luminosity for 3Dcase ($0 < \theta < 10^\circ$)

$$E_{\text{dot}} = - \int_{\theta=\theta_0}^{\theta=\theta_1} \int_{\phi=0}^{\phi=2\pi} \sqrt{-g} T_t^r dA$$

$\theta_0=0$
 $\theta_1=10$

outflow power $14R_g, 60R_g$



Short time variability ($\Delta t \sim$ a few tens GM/c³) in electromagnetic components (green and pink):
 \Rightarrow possible origine for flares in blazars (on axis observer),

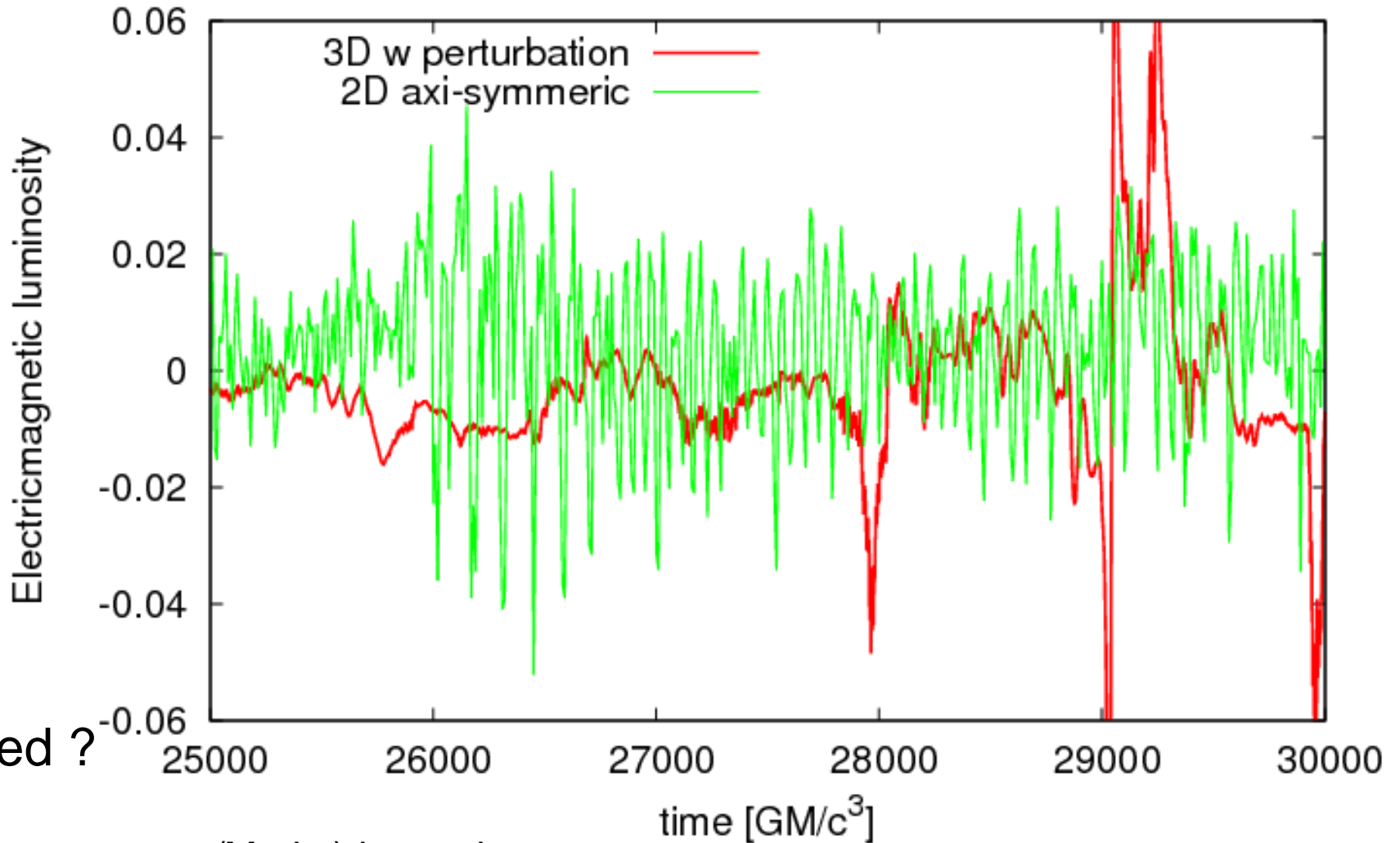
Blandford-Znajek process

Electricmagnetic power at and around event horizon

$$E_{\text{dot}} = - \int_{\theta=\theta_0}^{\theta=\theta_1} \int_{\phi=0}^{\phi=2\pi} \sqrt{-g} T_t^r dA$$

Electromagnetic components in T^μ_ν
 Electricmagnetic luminosity at horizon

$\theta_0=0, \theta_1=\pi$



BZ powered ?

Efficiency (Ele-mag power/ M_{dot}) is good for 2D case.

BZ flux v.s. EM flux @ horizon (1)

BZ1977, McKinney & Gammie2004

Radial electric-magnetic flux is described as

$$F_E^{EM}(r, \theta) = -2(B^r)^2 \omega r \left(\omega - \frac{a}{2r} \right) \sin^2 \theta - B^r B^\phi \omega (r^2 - 2r + a^2) \sin^2 \theta$$

@ event horizon

$$r = r_H = 1 + \sqrt{1 - a^2}$$

$$F_E^{EM}(r = r_H, \theta) = 2(B^r)^2 \omega r_H (\Omega_H - \omega) \sin^2 \theta$$

$$\Omega_H = \frac{a}{2r_H}$$

Rotation frequency
of BH

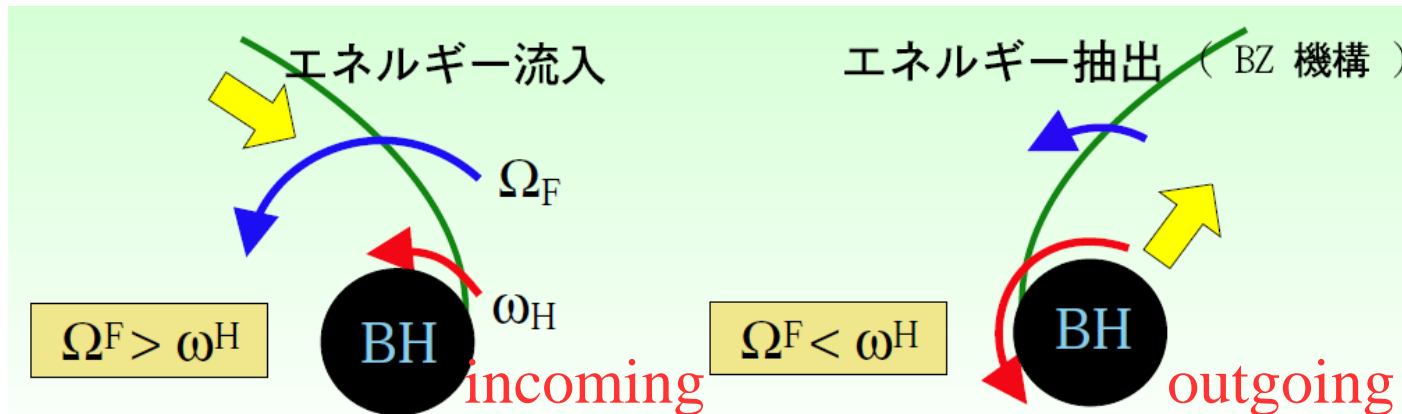
$$\omega = -\frac{F_{tr}}{F_{\phi r}} = -\frac{F_{t\theta}}{F_{\phi\theta}}$$

Rotation frequency of EM
field

$$\omega = -\frac{F_{tr}}{F_{\phi r}} = -\frac{b^\theta u^\phi - b^\phi u^\theta}{b^t u^\theta - b^\theta u^t}$$

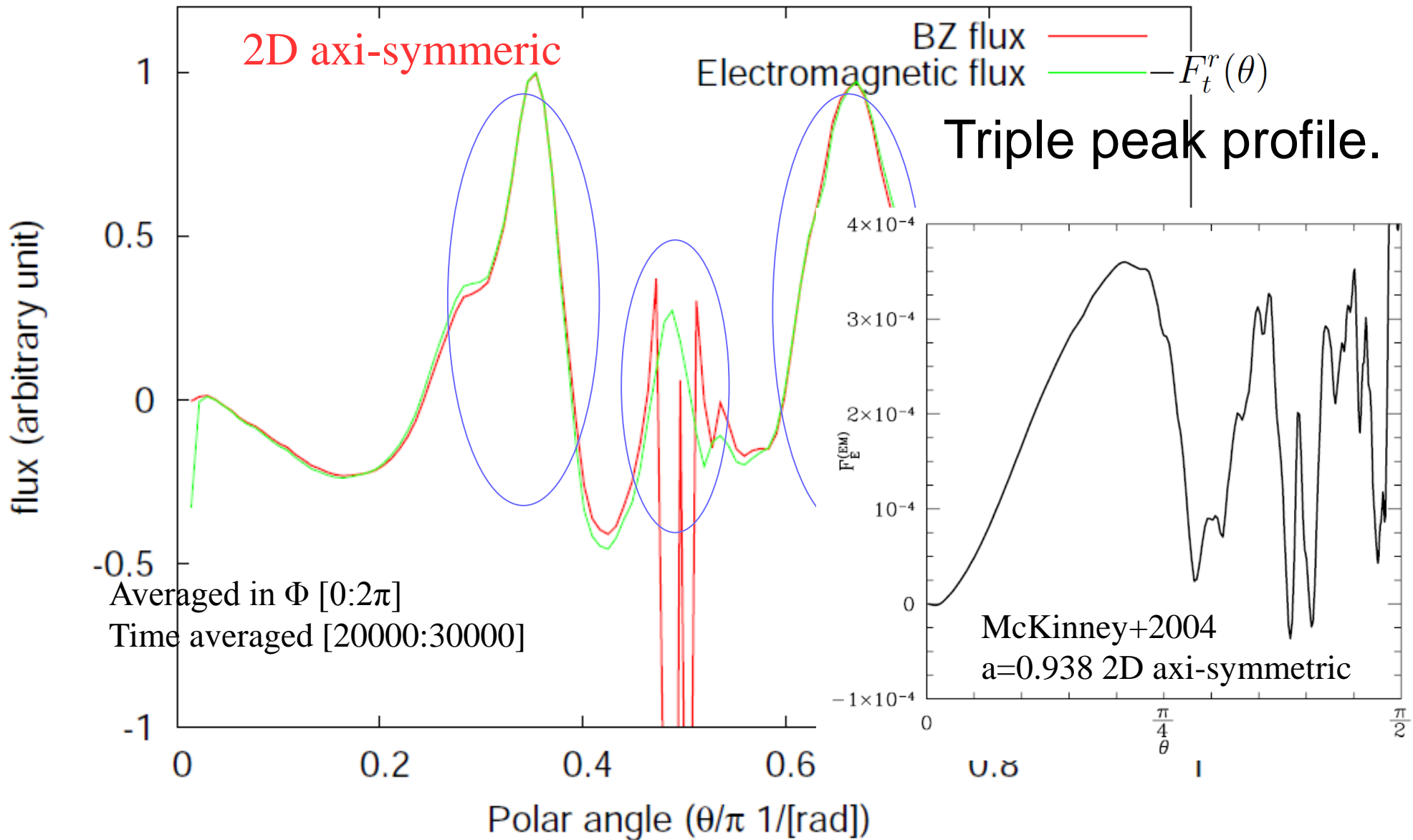
$$\omega = -\frac{F_{t\theta}}{F_{\phi\theta}} = -\frac{b^r u^\phi - b^\phi u^r}{b^t u^r - b^r u^t}$$

$0 < \omega < \Omega_H \Rightarrow$ outgoing flux



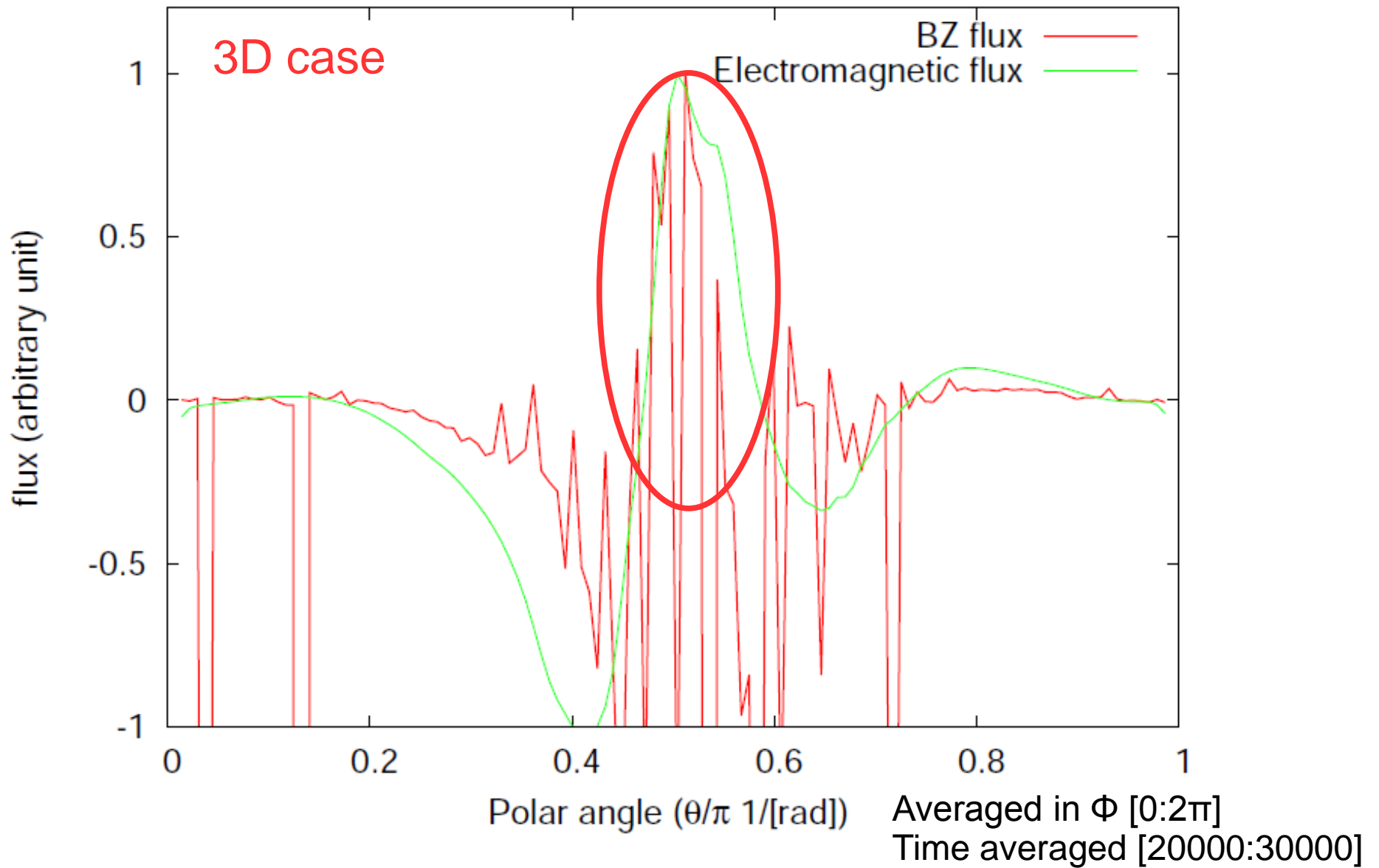
From Takahashi's
(AUE) slide

BZ flux v.s. EM flux @ horizon (2)



For 2D axi-symmetric case, time-averaged BZ flux is in good agreement with electromagnetic flux at horizon.

BZ flux v.s. EM flux @ horizon (3)



Electromagnetic flux is roughly good agreement with BZ flux.
Outgoing flux is concentrated around equator.

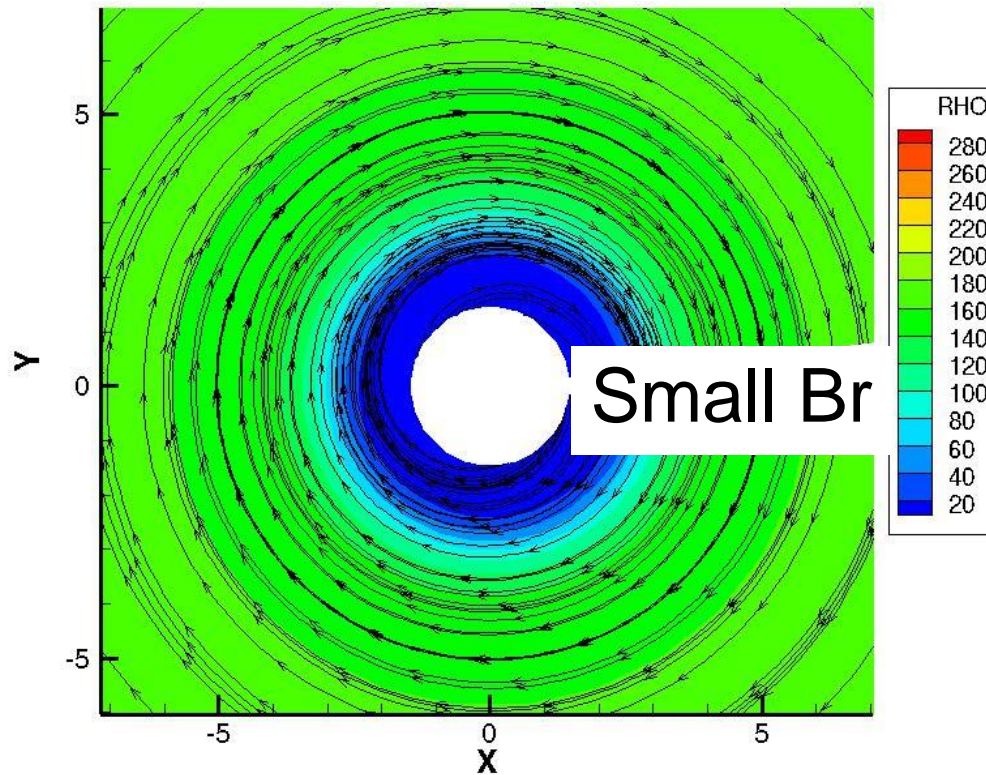
B-Filed line @equator

$$F_E^{EM}(r = r_H, \theta) = 2(B^r)^2 \omega r_H (\Omega_H - \omega) \sin^2 \theta$$

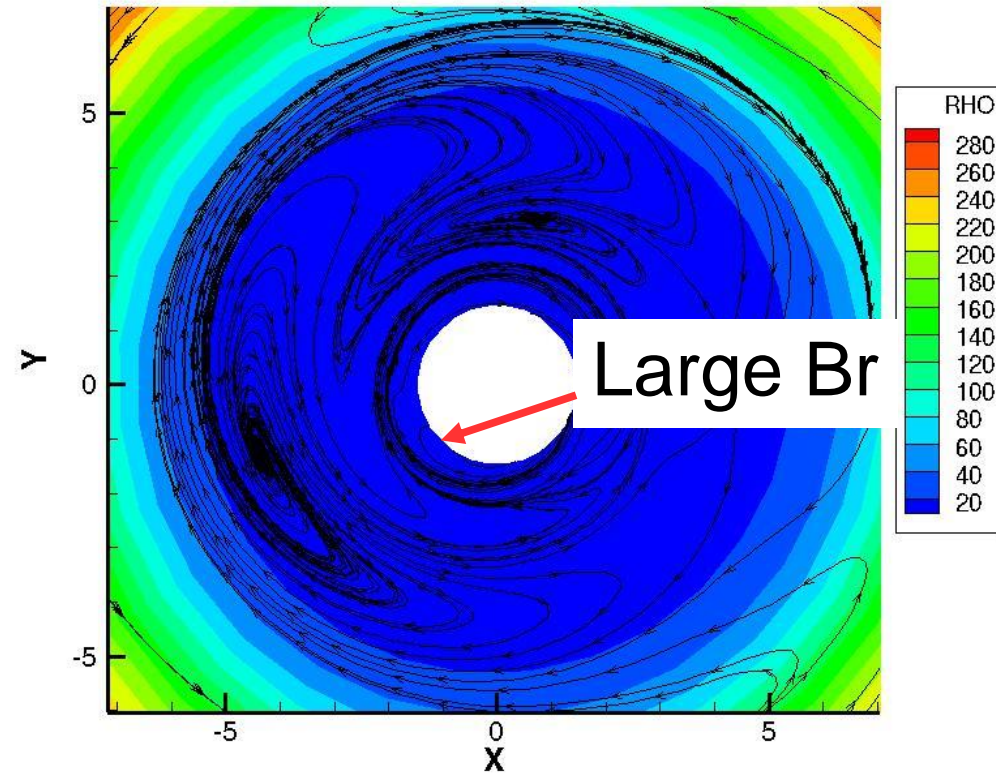
2D Axis-symmetric case
Axisymmetric

3D case

t=25000 [R_g/c]



t=25000 [R_g/c]



Tilt angle of B-field line to black hole surface normal is large.

Small Br

Tilt angle of B-field line to black hole surface normal is large.

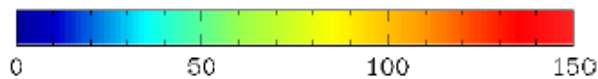
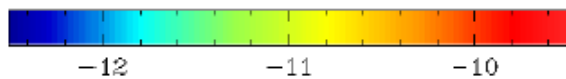
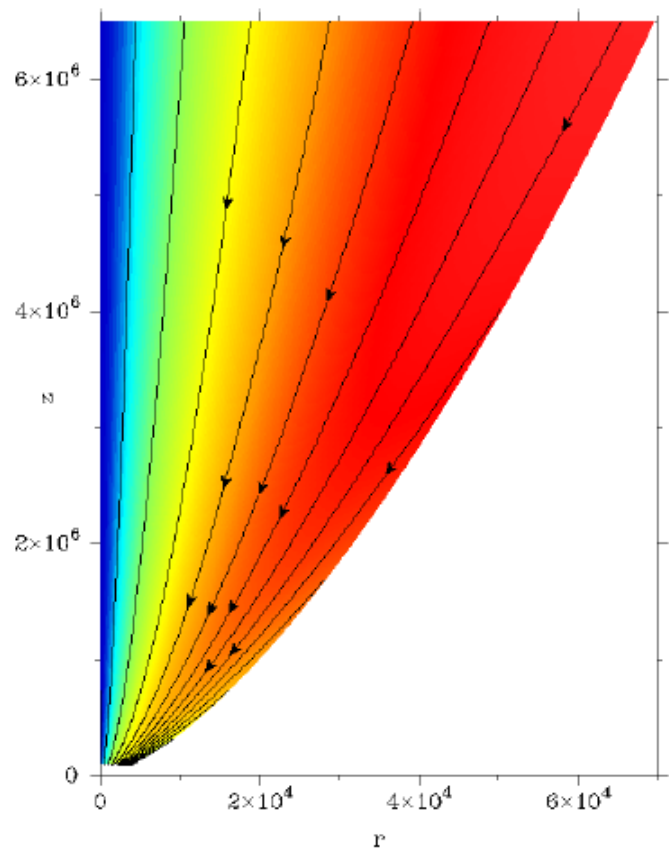
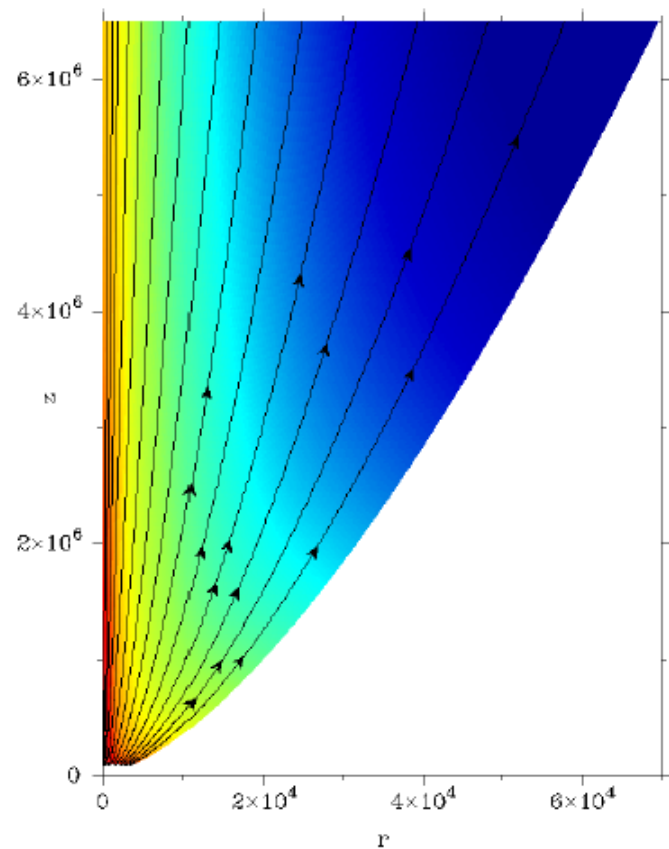
Br large in Local

Bulk Acceleration

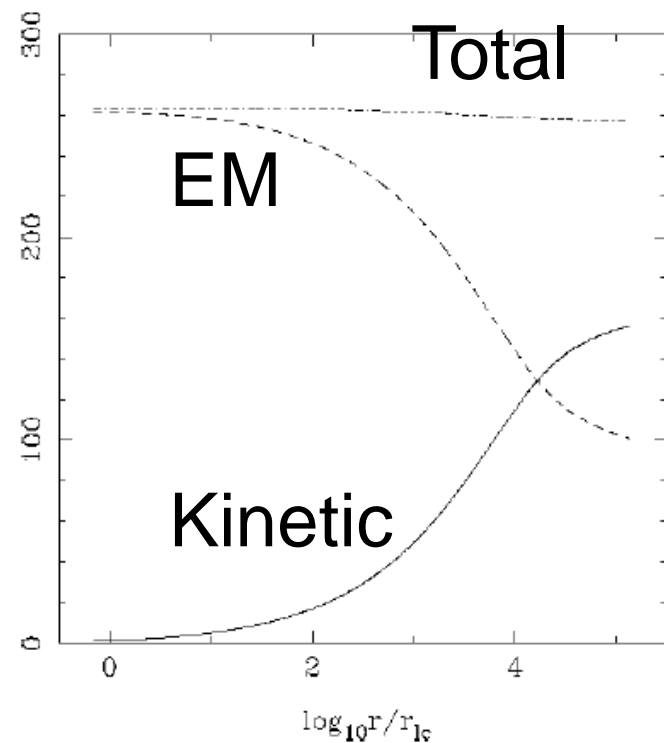
How to convert magnetic energy
to kinetic energy ?

$\rho\Gamma$, B-filed line

Γ , current

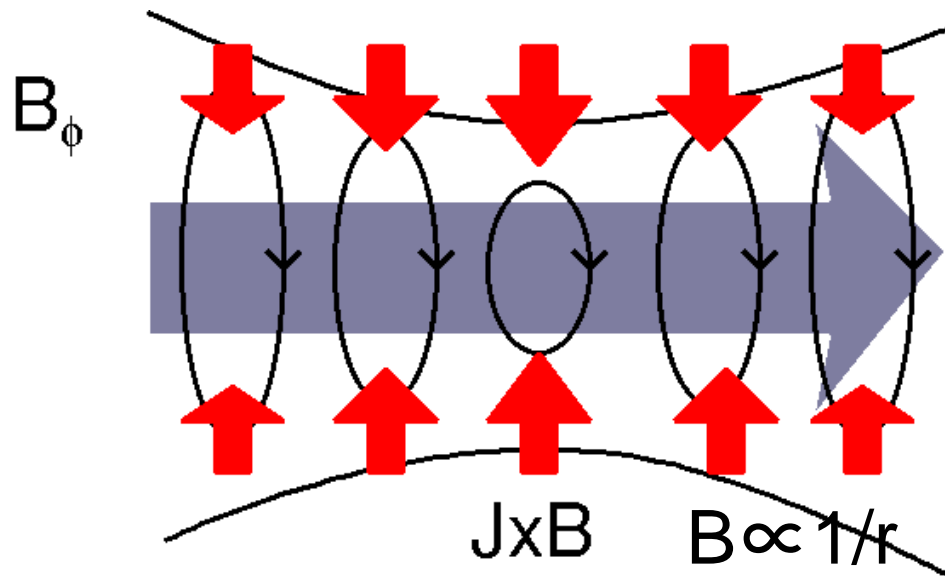
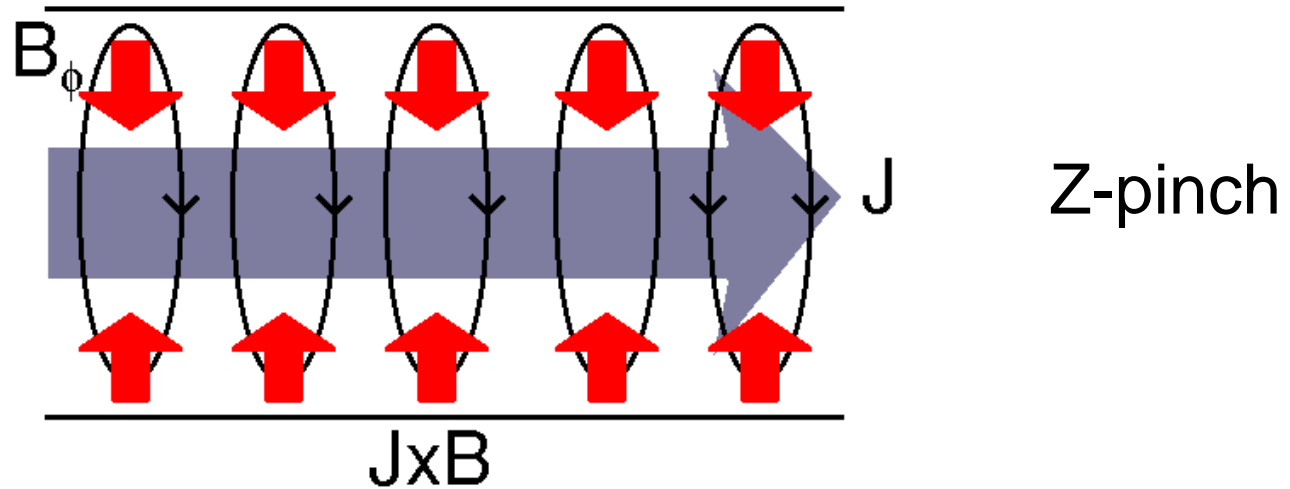


$$r_{lc} \equiv c/\Omega$$

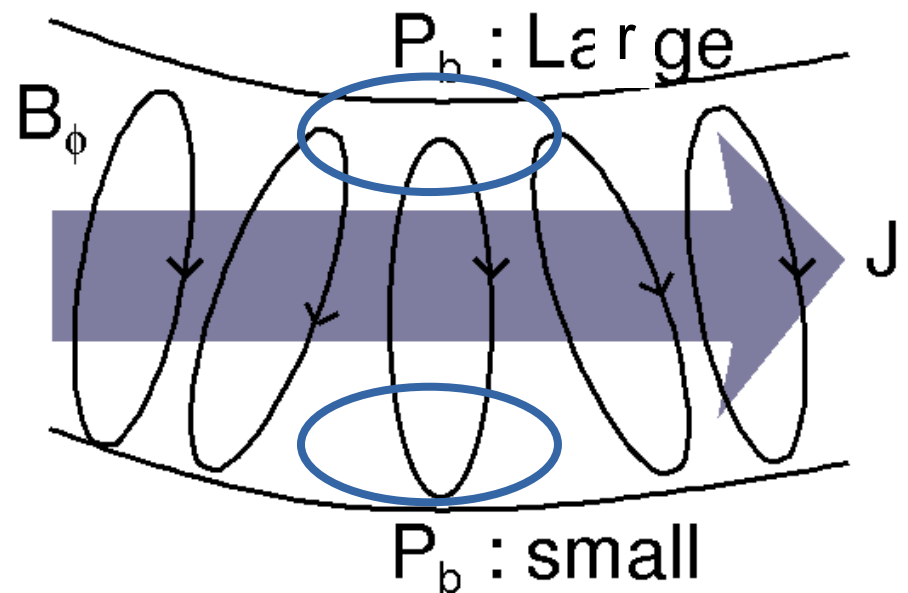


Good conservation
in enthalpy

MHD instability (current driven instability)

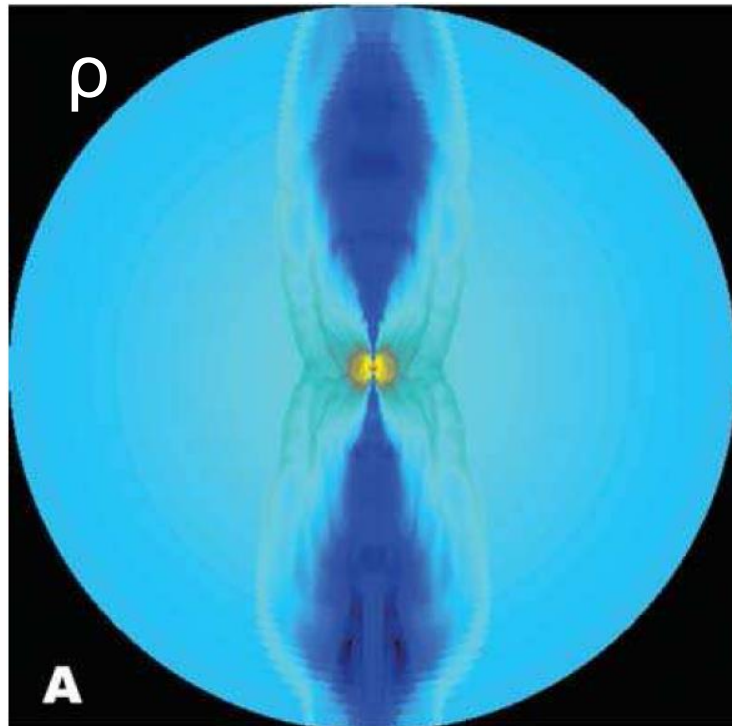


Sausage instability
 $m=0$ mode



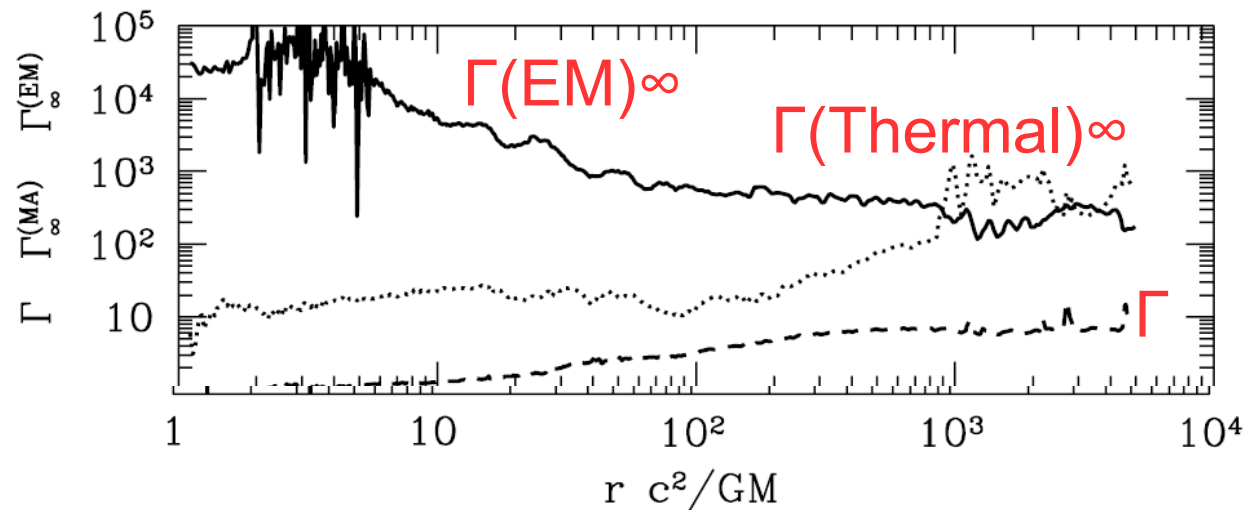
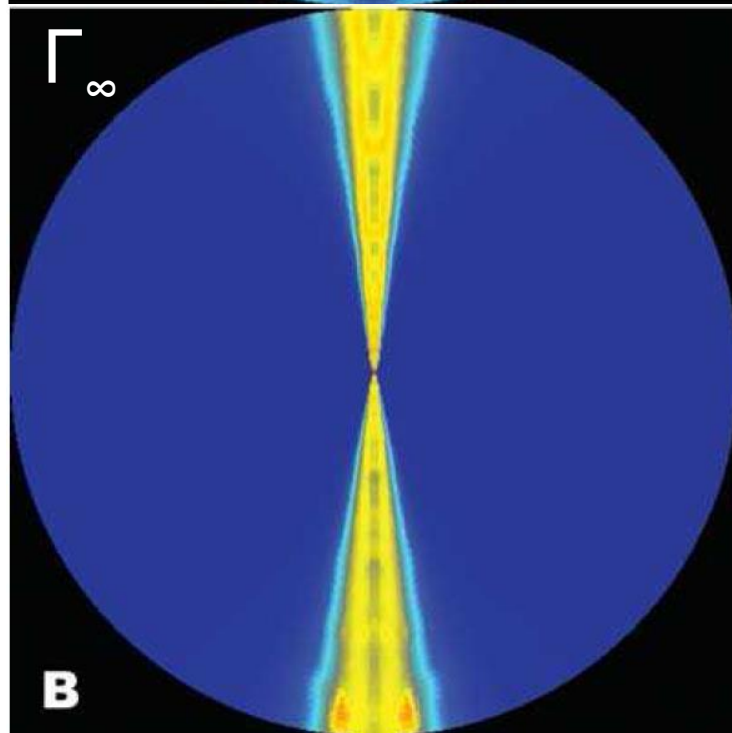
Kink instability
 $m=1$ mode

Sausage instability (m=0 mode)



$10^4 R_g$

- 2D GRMHD simulation
- Sausage (pinch) instability grows up.
- It enhances oscillation and generates waves, converting magnetic energy into lateral kinetic energy
- Finally shock dissipation



McKinney 2006 MNRAS 368 (2006)

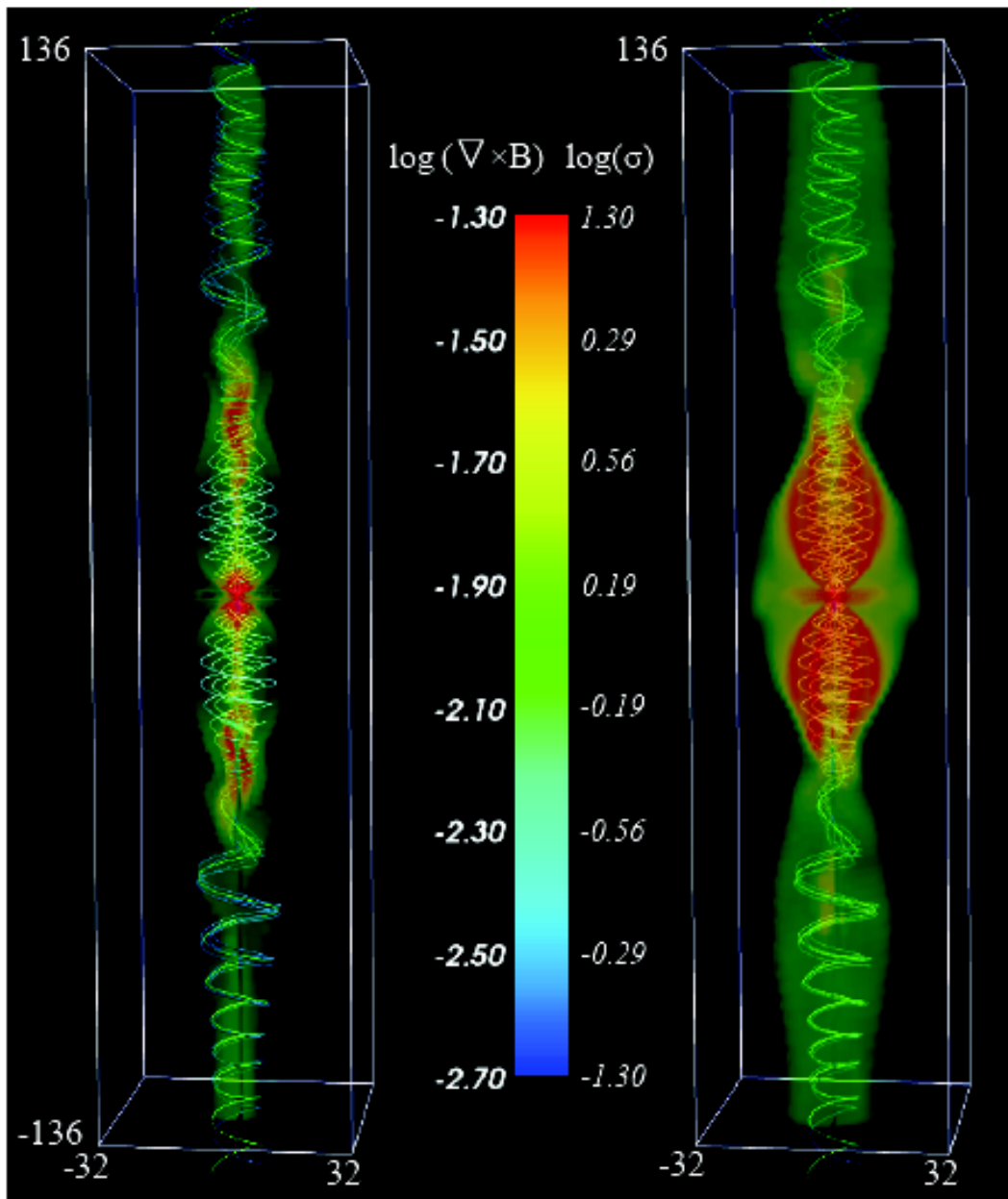
Kink instability (m=1 mode)

- Magnetized jet propagation in large scale.
- Kink instability (m=1 mode) grows up.
- Dissipation (reconnection) happens. Then magnetic energy is converted to thermal and kinetic energy.

Kink instability triggers small angle reconnection
(Drenkhahn 2002,
Drenkhahn & Spruit 2002)

3D RMHD simulation
of magnetized jets propagation
in massive star.

(Bromberg & Tchekhovskoy 2015)

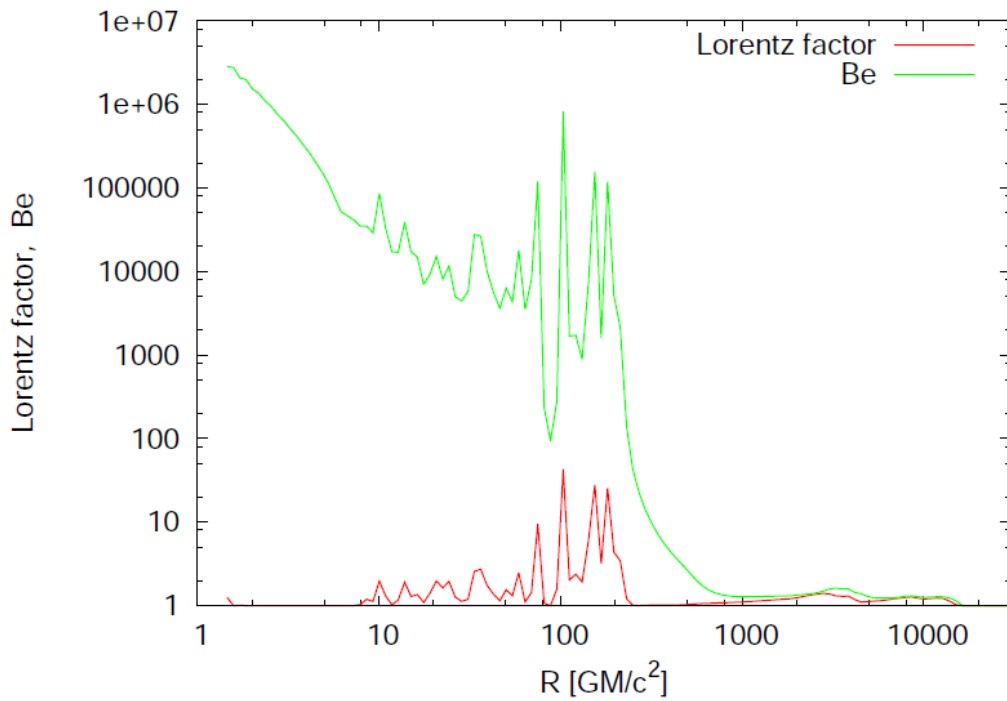


Left: $\log_{10} [\text{rot}(\nabla \times \mathbf{B})]$ (conduction current)

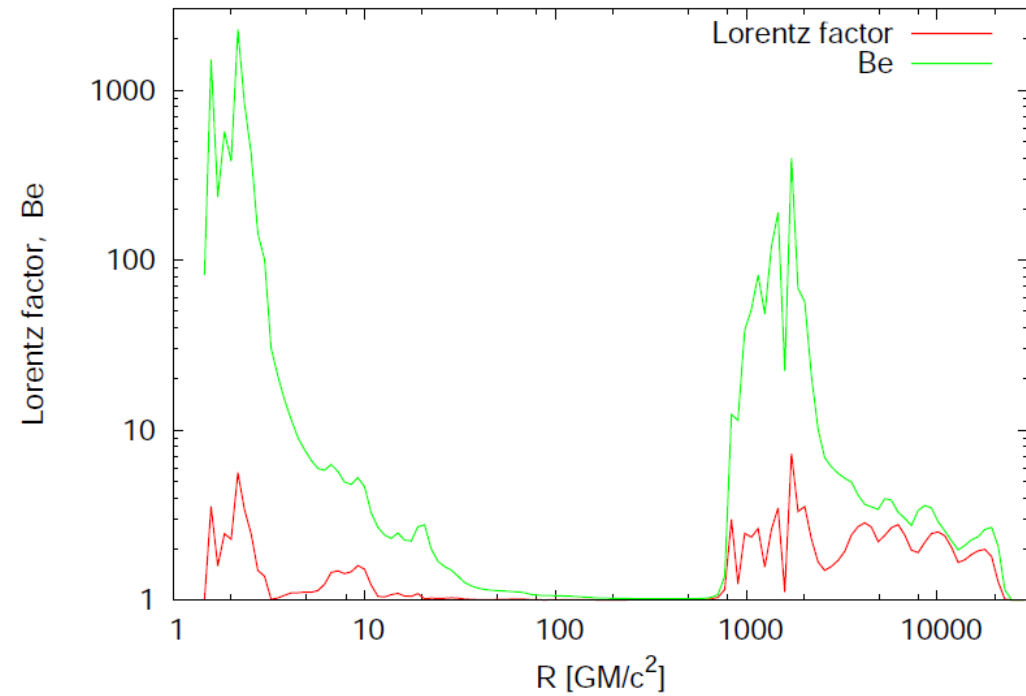
Right: $\log_{10} [\sigma]$

Lorentz factor, Be along polar axis

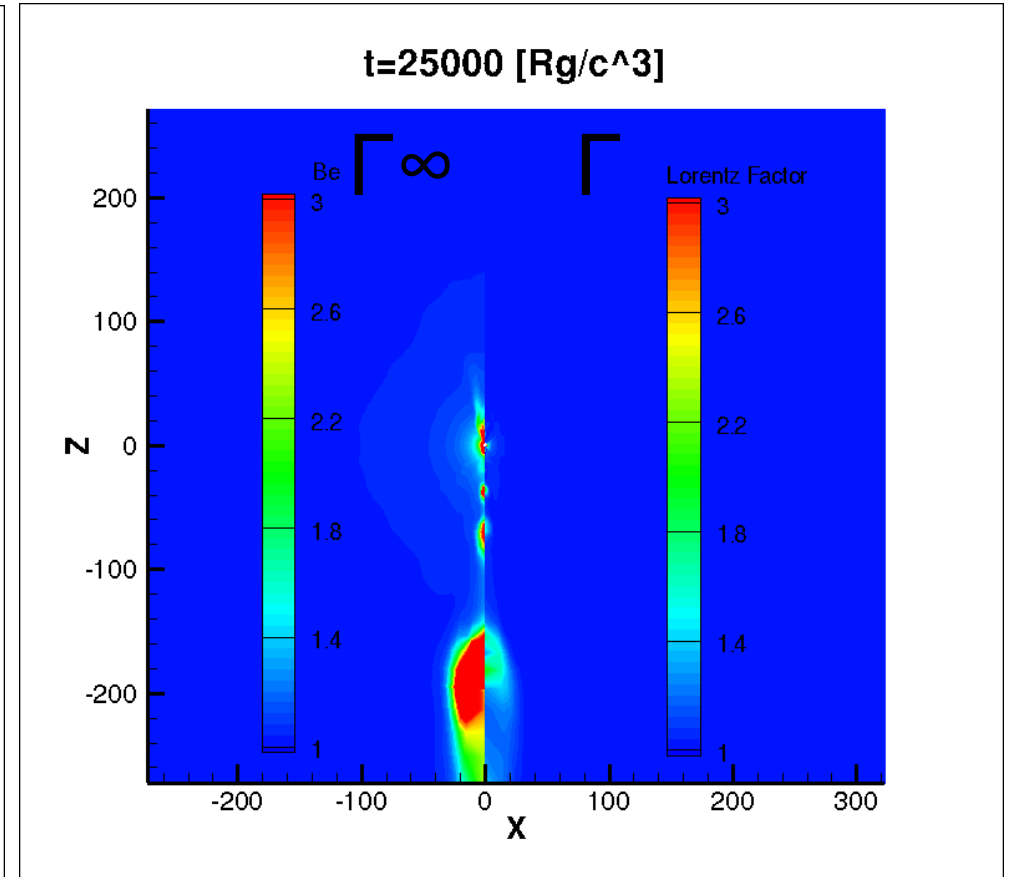
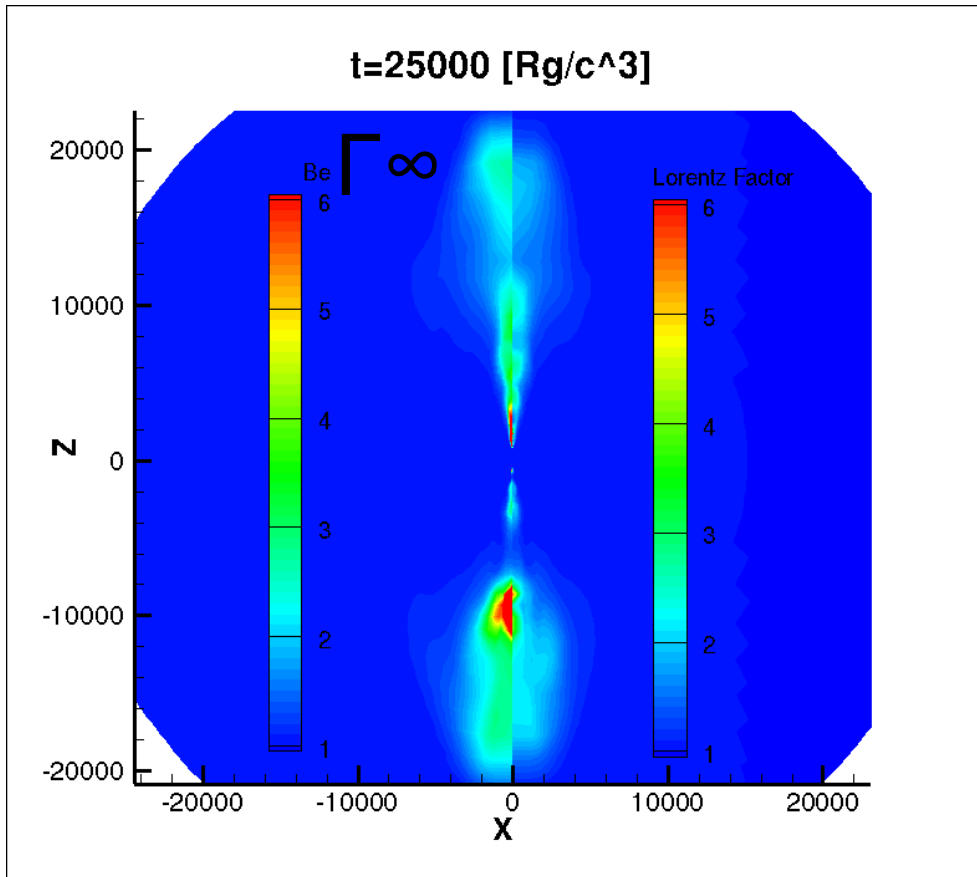
2D RUN



3D RUN



Bulk acceleration $\Gamma \sim 2$

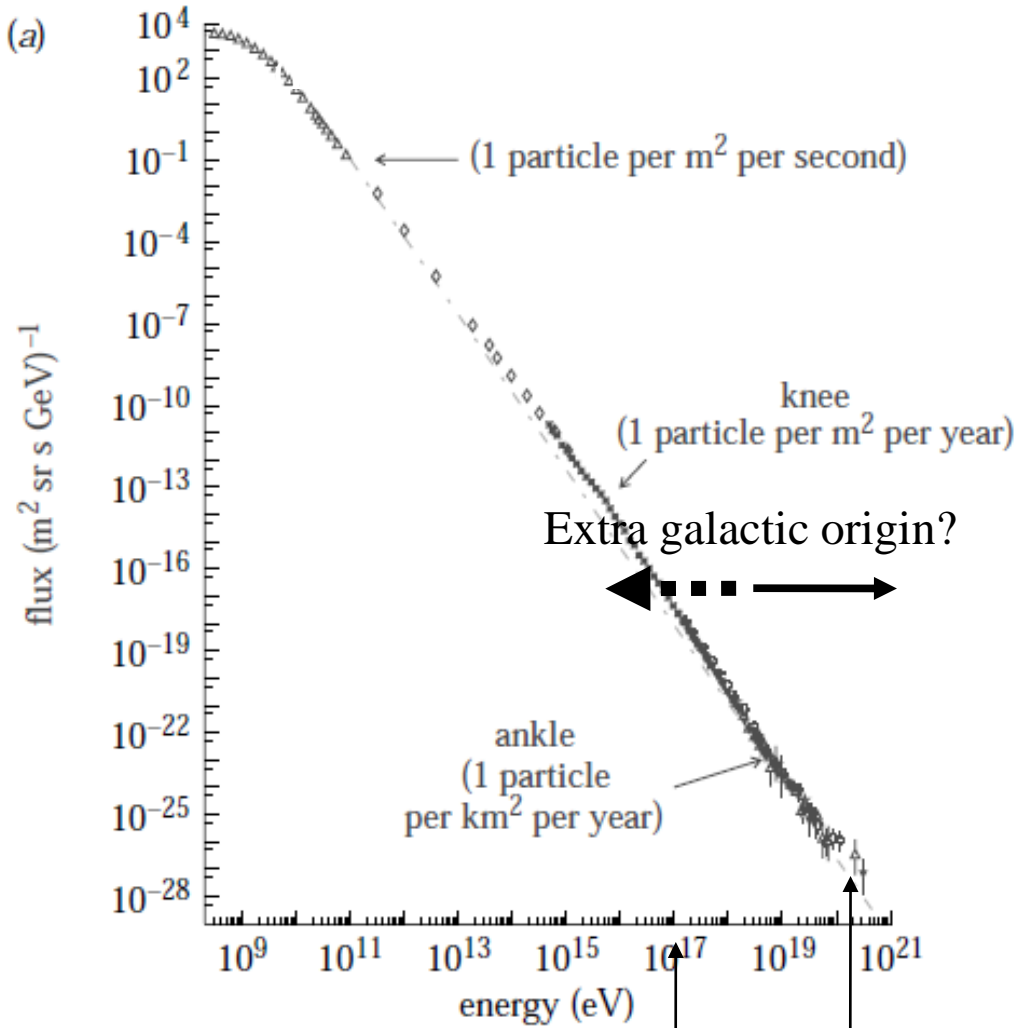


Structures are resolved by only 1-2 grids.
Higher resolution calculation necessary to see MHD instability
and bulk acceleration.

Mizuta+ in prep.

Particle acceleration by wakefield acceleration

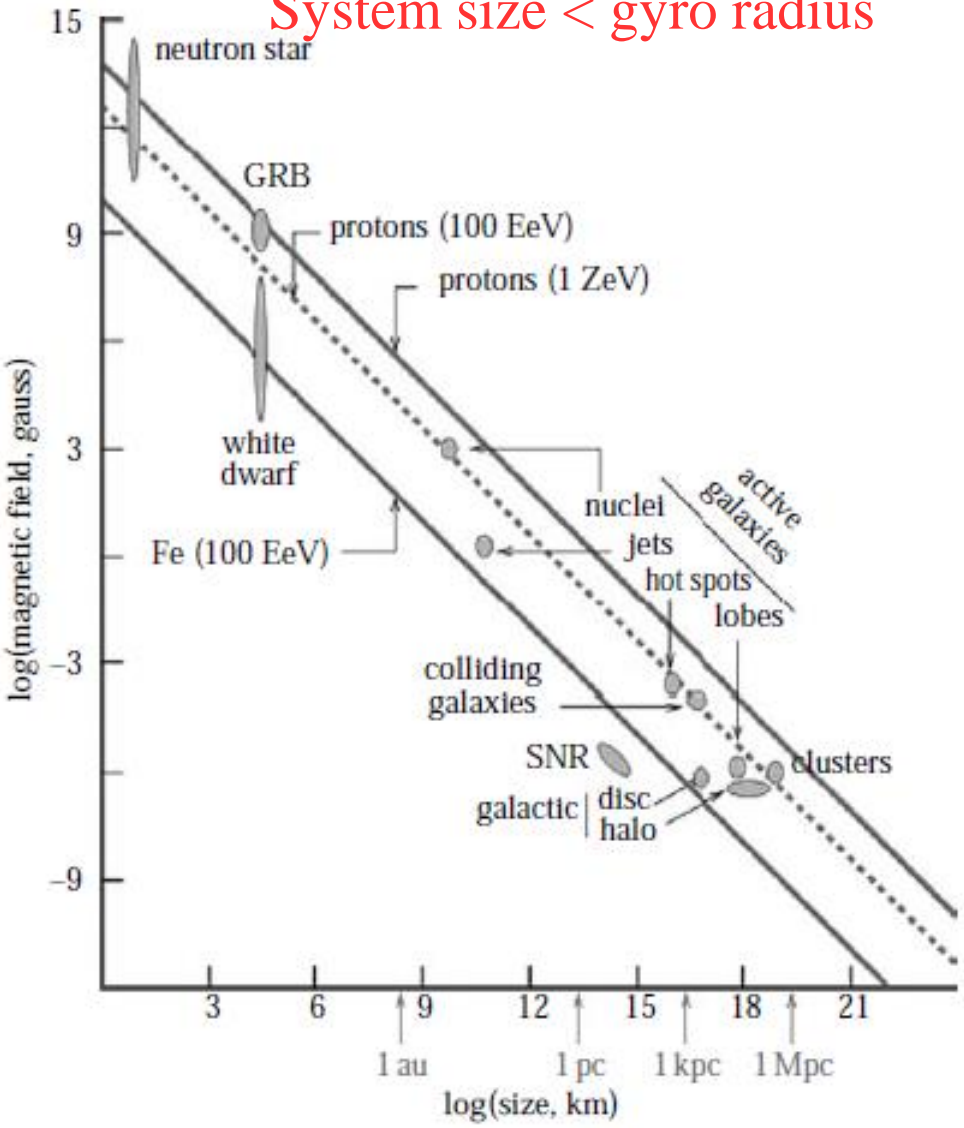
Cosmic-ray up to $\sim 10^{20}$ eV



LHC(14TeV Center-of-mass system)

Hillas plot : $E_{\text{max}} \sim Z e B R$

System size < gyro radius



AGN : UHECR accelerator ?

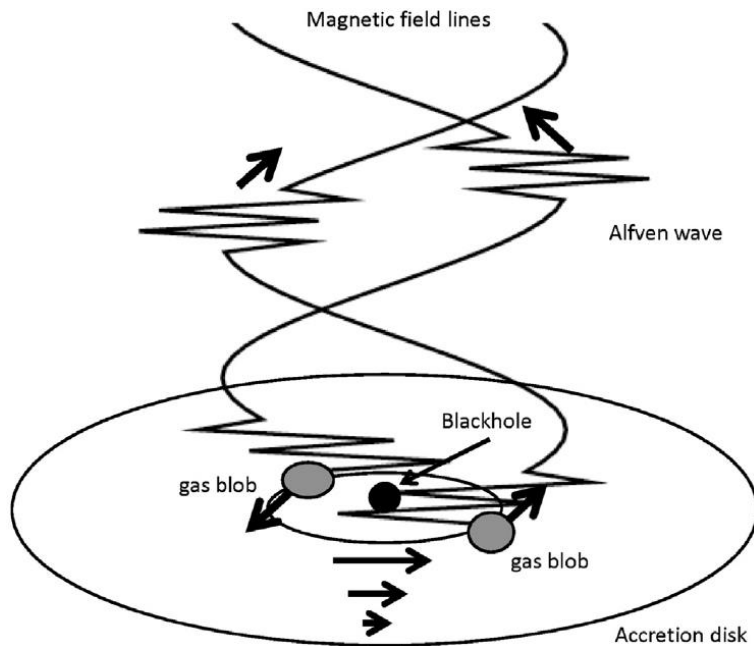
Wakefield acceleration model (excited by Alfvén wave)

Intense laser pulse => strong Alfvén wave ($v_A \sim c$, **transverse wave**)

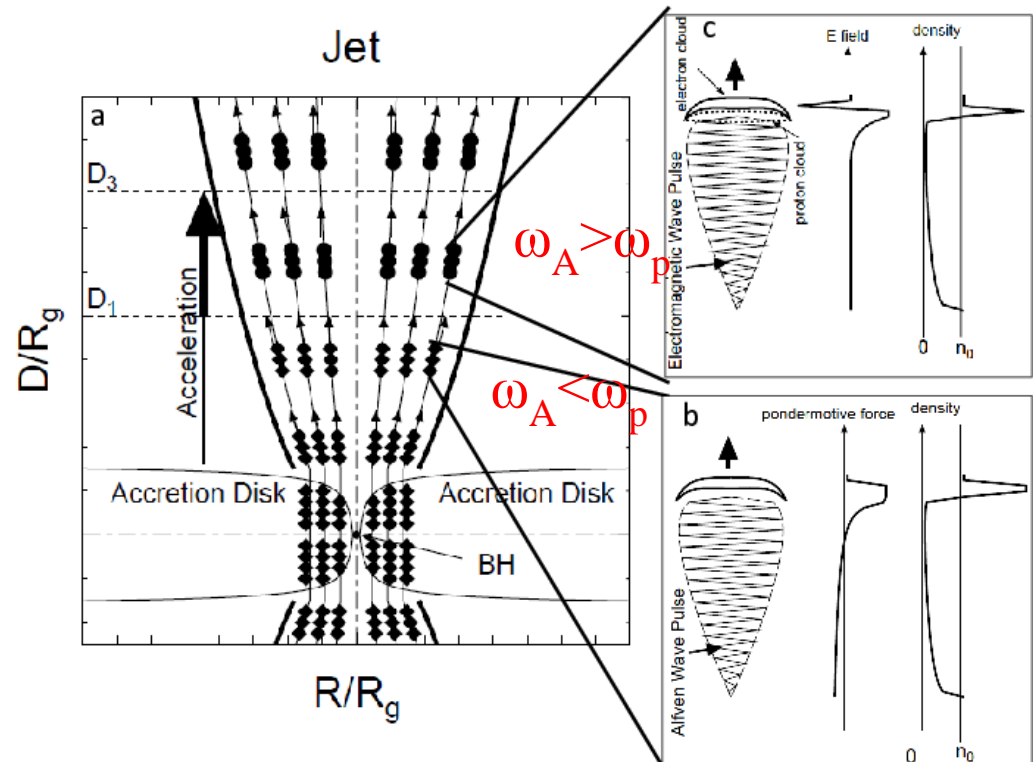
Alfvén waves excited in the accretion disk propagates into the outflows. If magnetic field is enough high, relativistic Alfvén waves is possible.

$$a = \frac{eE}{m_e \omega_{AC}} = 2.3 \times 10^{10} \left(\frac{\dot{M}}{0.1 \dot{M}_c} \right) \left(\frac{M_{BH}}{10^8 M_\odot} \right) \gg 1$$

nonlinear & relativistic Alfvén mode Standard-disk (Shakura & Sunyaev (1973) is assumed)

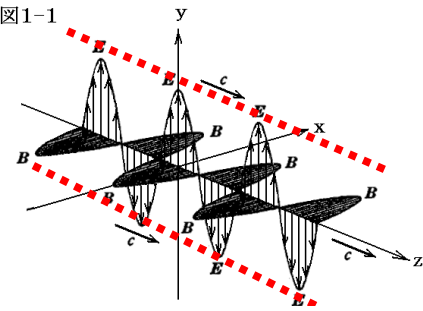


Ebisuzaki & Tajima 2014

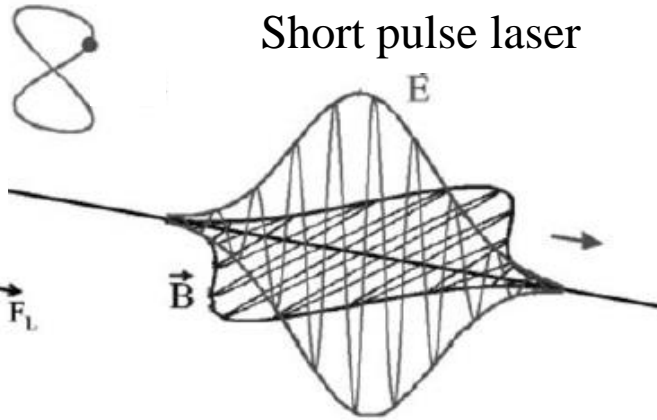


Wakefield acceleration (Tajima & Dawson PRL 1979)

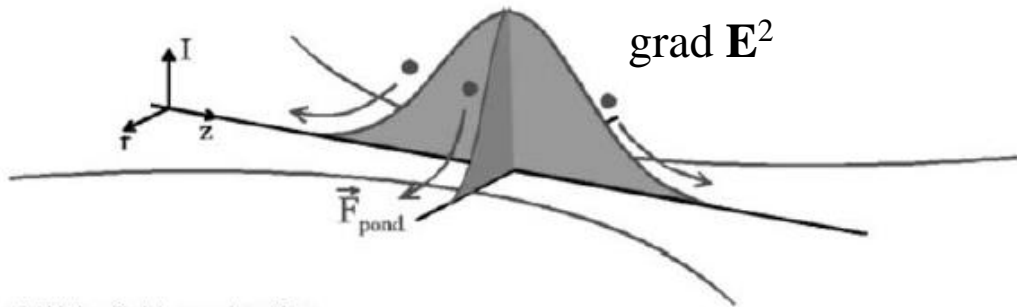
Acceleration mechanism by interaction between wave and plasma.



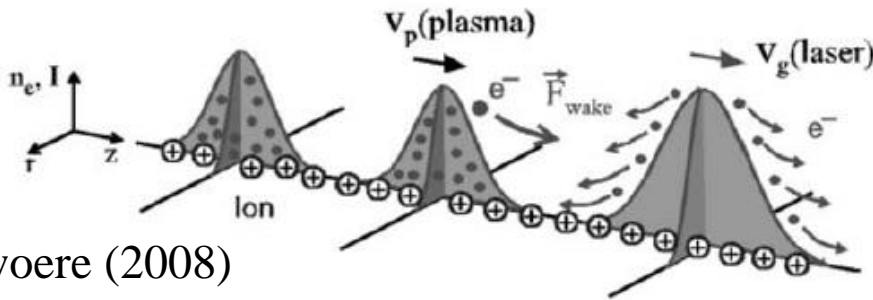
Laser plasma Interaction
 \Rightarrow 8 shape motion.



b) Ponderomotive force



c) Wake field acceleration



Schwoere (2008)

$$\mathbf{F} = q \left(\mathbf{E} + \frac{\mathbf{v}}{c} \times \mathbf{B} \right)$$

Oscillation of Electric field \Rightarrow **v** (oscillation up, down)
 $\mathbf{v} \times \mathbf{B}$ force \Rightarrow **oscillation forward and backward.**
 $|\mathbf{v}| \sim c \Rightarrow$ large amplification motion by $\mathbf{v} \times \mathbf{B}$. (**8 shape motion**).

If there is gradient in E^2 , charged particles feel the force towards less E^2 side. = Ponderomotive force

Effective acceleration for $I \sim 10^{18} \text{W/cm}^2$ (relativistic intensity).
 – acceleration efficiency 10 GeV/m (100-1000 higher than normal accelerators.,
Electrons: ~GeV, Ions : a few tens MeV

Relativistic Alfvén wave can be applied to Wakefield acceleration.

Takahashi+2000, Chen+2002 (for short GRBs : NS-NS merger)

Lyubarusky 2006, Hoshino 2008 (wakefield acc. @ relativistic shock)

Initial Condition

Initial condition for GRMHD simulations of accretion flows onto BHs

Most of GRMHD simulations of accretion flows onto BHs adopt an equilibrium solution that is Fishbon-Moncrief solution (1976). The solution includes 6 free parameters.

Imposing weak magnetic field and/or weak perturbations, the simulations try to find new quasi-steady state.

Recently Penna, Kulkarni, Narayan (2013) proposes new solution which is more realistic.

Fishbon-Moncrief equilibrium solution (1976) –(1)

Assumption –

steady state, axis-symmetric

$u^r = u^\theta = 0$: 4-velocity

ignore self gravity of disk


procedure : assume angular momentum distribution

⇒ find velocity field

⇒ find thermodynamic quantities

4-velocity has 4 components but only 3 of them are free Parameters due to normalization of 4-velocity.
 Since $u^r = u^\theta = 0$ is assumed,


$l_* \equiv -u^t u_\phi = \text{const}$: Fishbon-Moncrief solution



$$(u^t)^2 = \frac{g_{\phi\phi} + \sqrt{g_{\phi\phi}^2 + 4(g_{t\phi}g_{t\phi} - g_{tt}g_{\phi\phi})l_*^2}}{2(g_{t\phi}g_{t\phi} - g_{tt}g_{\phi\phi})} \quad u^\phi = \frac{-l_* - g_{t\phi}u^t}{g_{\phi\phi}u^t}$$

$l \equiv -u_\phi / u_t = \lambda^c$: Chakarabarti (1985)

=const : Kozlowski(1978),
 Komissarov (2006) with toroidal B-field



$$\Omega(r, \theta) = -\frac{g_{t\phi} + l g_{tt}}{g_{\phi\phi} + l g_{t\phi}}$$

$$u^t(r, \theta) = (-g_{tt} - 2\Omega g_{t\phi} - \Omega^2 g_{\phi\phi})^{-1/2}$$

$$u^\phi(r, \theta) = u^t \Omega$$

Fishbon-Moncrief solution (1976) –(2)

Relativistic Euler Eq. $\nabla_{\mu} T^{\mu\nu} = 0$,

Using assumptions of steady state and axis-symmetry

$$\frac{p_{,i}}{\rho h} = -(\ln |u_t|)_{,i} + \frac{\Omega}{1 - l\Omega} l_{,i} \quad (i=r, \theta)$$

Pressure gradient, gravitational potential,
and centrifugal force balance

If the gas is barotropic $\rho = \rho(p)$ the surfaces of Ω , l , const coincide.

(relativistic von Zeipel's theorem, Abramowicz(1971))

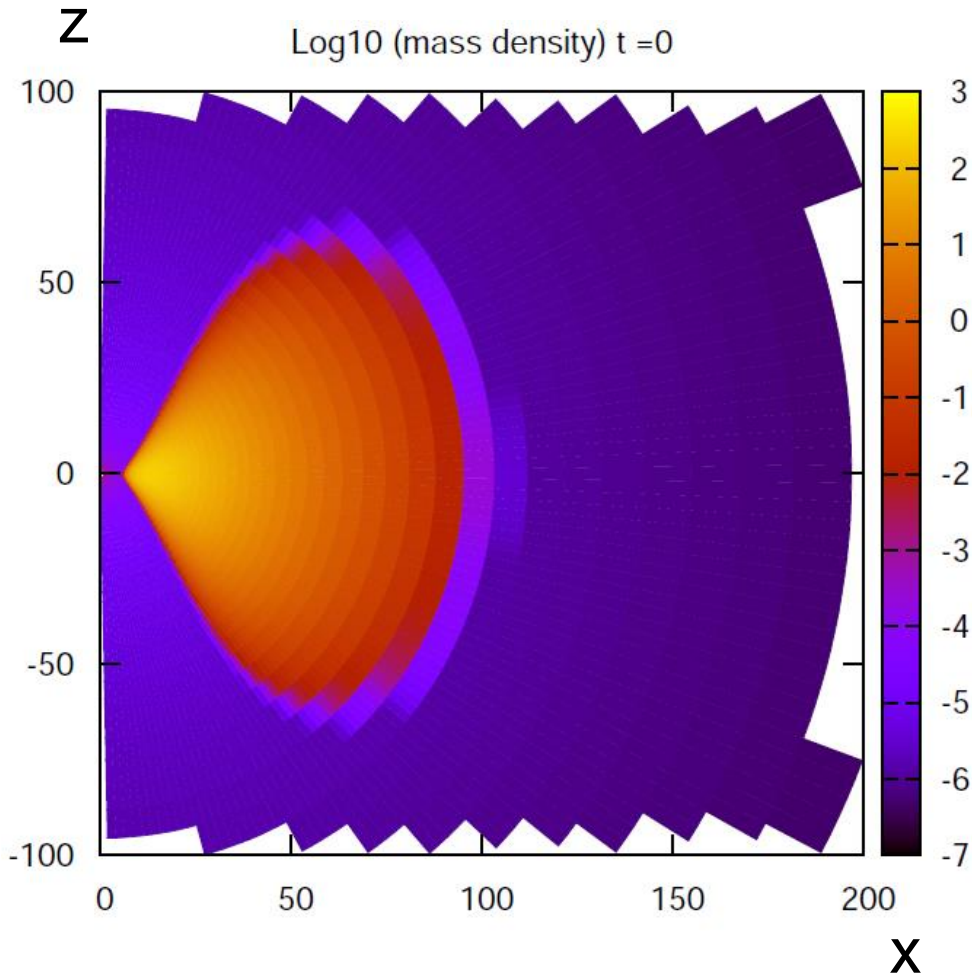
Ω , l const surface is so-called relativistic von Zeipel cylinder.

Assuming EOS and disk inner edge radius r_{in} ,
pressure is derived by integrating balance equation.
 $P=0$ surface is disk edge.

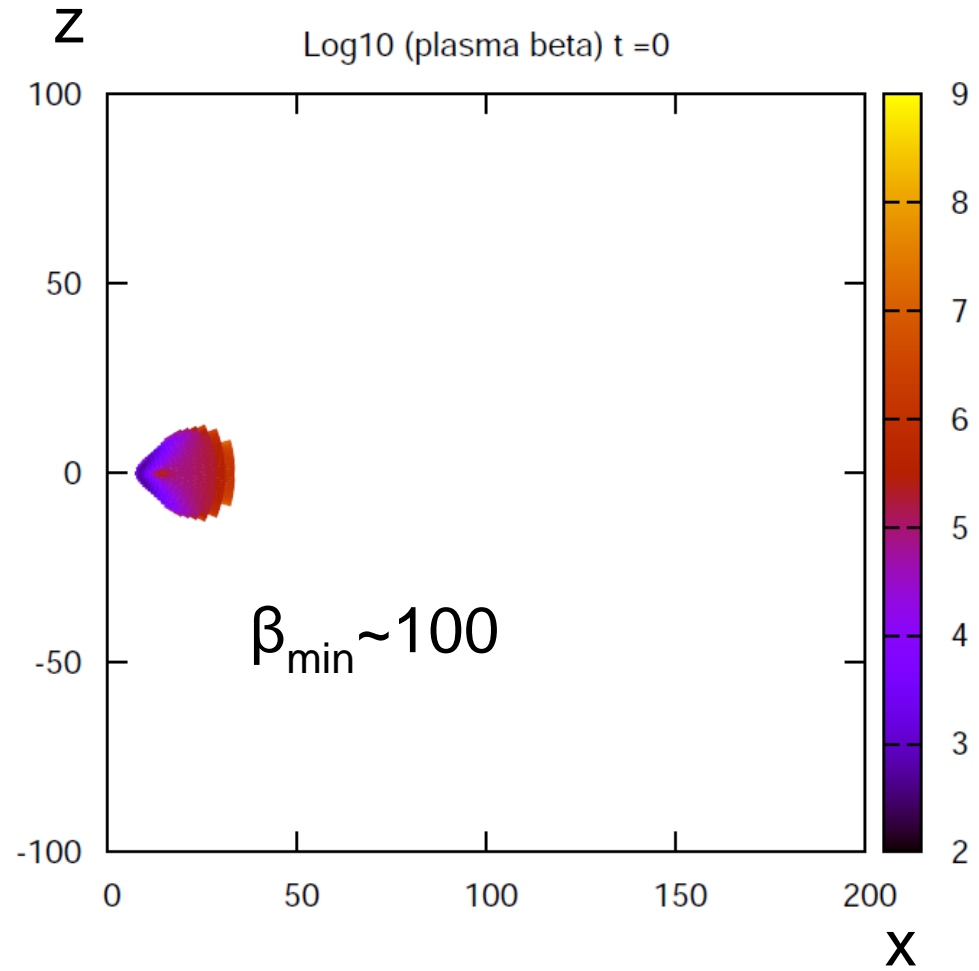
Fishbone-Moncrief solution (l^* : const) tends to be
geometrically thick disk.

Initial Condition

Log10 (Mass density)



Log10(Pgas/Pmag)



Fisbone-Moncrief (1976) solution : $a=0.9$,

$$A_{\phi} \propto \max [\rho / \rho_{\max} - 0.2, 0]$$

$$l_* \equiv -u^t u_{\phi} = \text{const} = -4.45, r_{\text{in}} = 6.$$

New torus solution : Penna, Kulkarni & Narayan (2013)

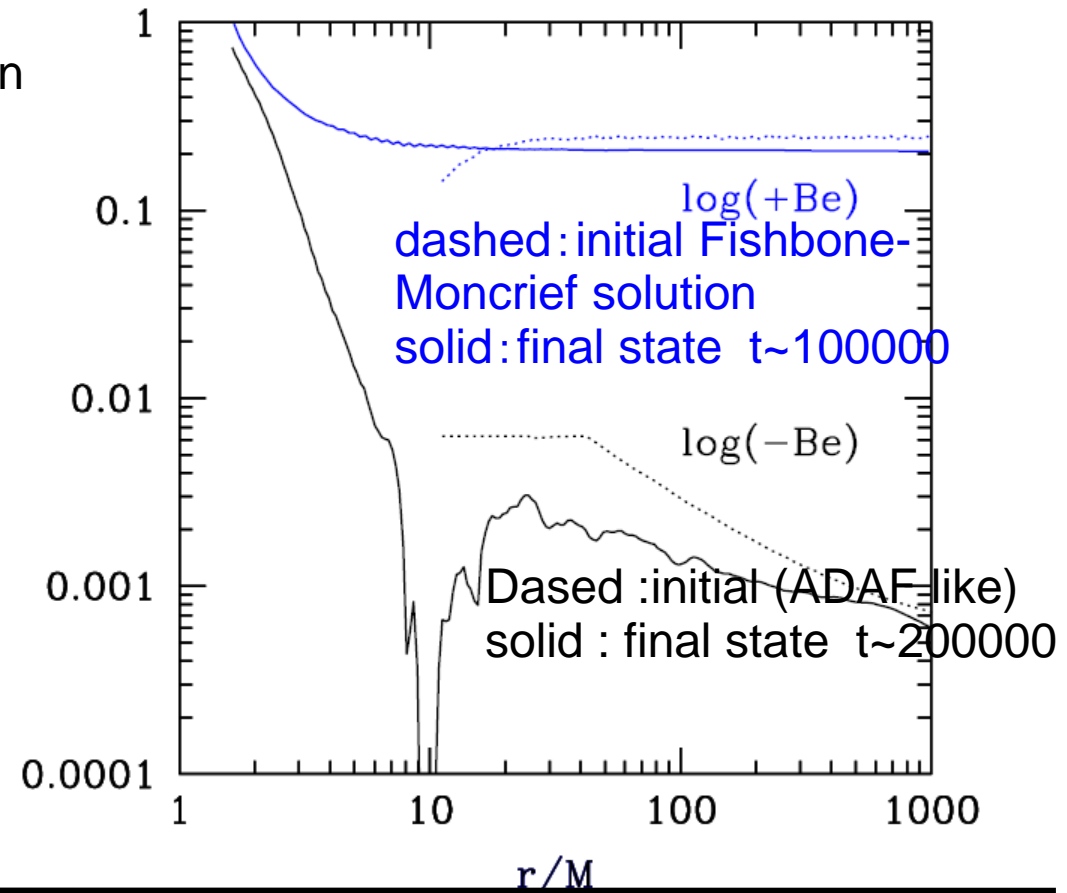
• Does the system forget initial condition, when enough time has passed ? \Rightarrow NO !

• Bernoulli constant $Be \equiv -hu_t - 1$
 Be distribution strongly depends on its initial distribution.

Be > 0 unbounded
 Be < 0 bounded

• Unbound flow @ t=0 can easily form an outflow.

• It is not easy to control Be constant in Fishbone-Moncrief solution



Similar with Keprelian specific angular momentum density distribution

λ : relativistic von Zeipel cylinder radius

$$\ell(\lambda) = \begin{cases} \xi \ell_K(\lambda_1) & \text{if } \lambda < \lambda_1 \\ \xi \ell_K(\lambda) & \text{if } \lambda_1 < \lambda < \lambda_2 \\ \xi \ell_K(\lambda_2) & \text{if } \lambda > \lambda_2. \end{cases}$$

$$\lambda^2 = -\ell(\lambda) \frac{\ell(\lambda)g_{t\phi} + g_{\phi\phi}}{\ell(\lambda)g_{tt} + g_{t\phi}}.$$

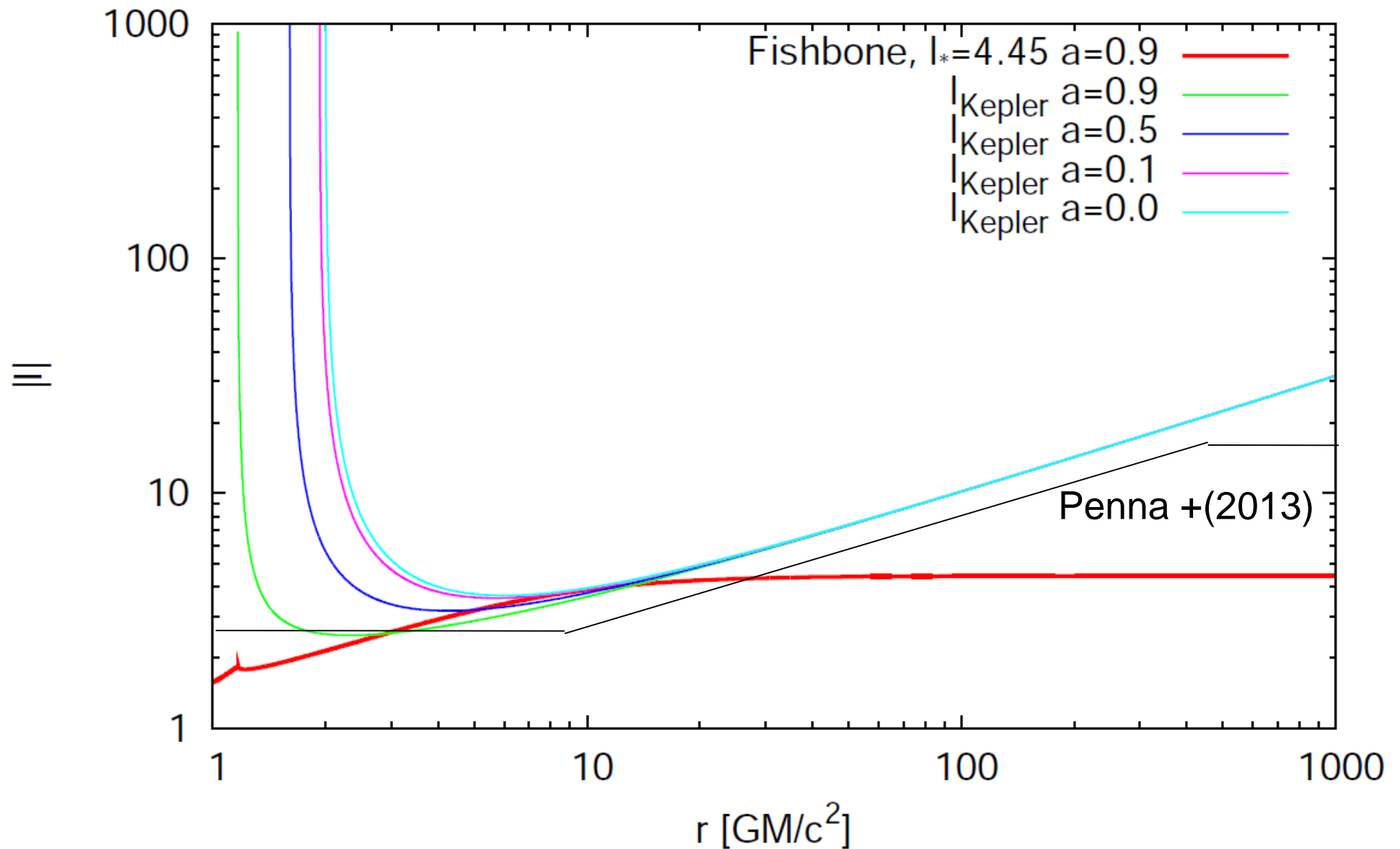
ℓ_K : specific angular momentum density @ equator
 $\xi \sim 1$ (strength parameter of roation)



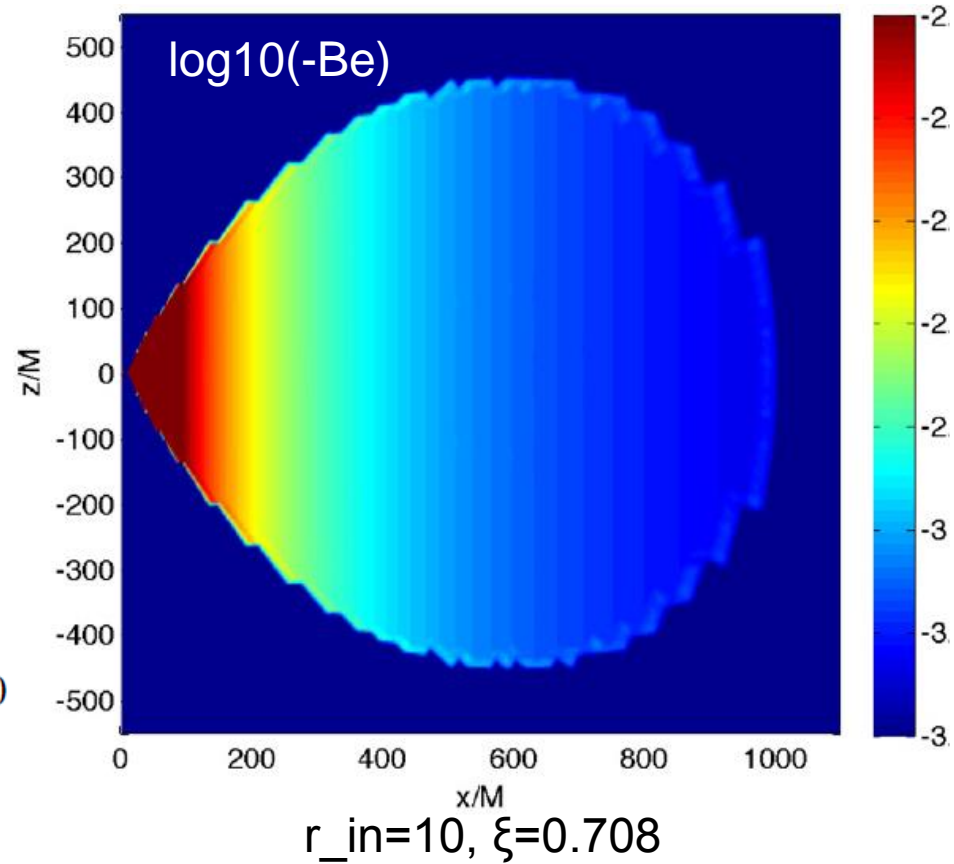
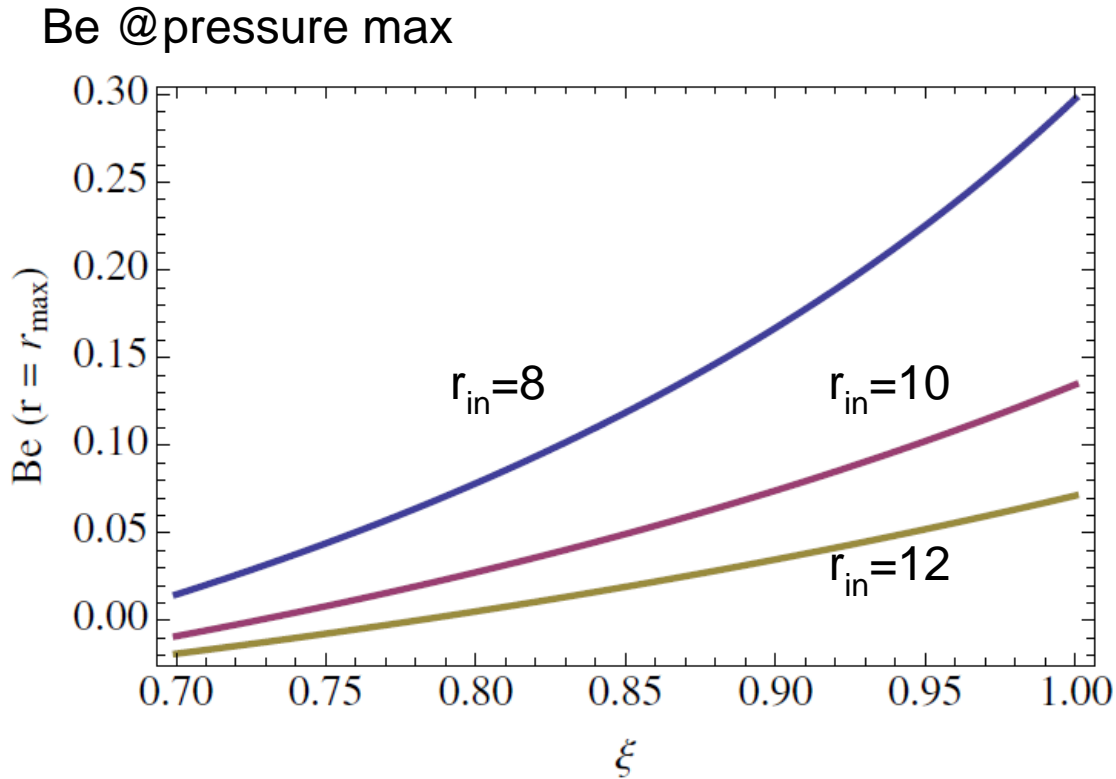
Disk outer edge can be far away ($R \sim 10000R_g$).
 Be distribution, and thickness of the disk can be independently controlled.

Specific Angular momentum density dis. @ equator

specific angular momentum for Keplerian orbit



Penna +(2013) equilibrium solution



$$\ell(\lambda) = \begin{cases} \xi \ell_K(\lambda_1) & \text{if } \lambda < \lambda_1 \\ \xi \ell_K(\lambda) & \text{if } \lambda_1 < \lambda < \lambda_2 \\ \xi \ell_K(\lambda_2) & \text{if } \lambda > \lambda_2. \end{cases}$$

Be < 0 (bounded) for $\xi \sim < 0.8$
 disk thickness can be controlled

Summary

2D & 3D GRMHD simulations of rotating BH+accretion disk

- B field amplification, saturation, dissipation
- Higher mass accretion rate for 3D than that in 2D case
- Electromagnetic flux @ horizon is consistent with BZ flux
- Higher resolution calculations are necessary to discuss bulk acceleration